Cracking the Skin Barrier: Liquid-Liquid Phase Separation Shines under the Skin

Alexa Regina Chua Avecilla[1] and Felipe Garcia Quiroz[1]

Central to forming and sustaining the skin's barrier, epidermal keratinocytes (KCs) fluxing to the skin surface undergo a rapid and enigmatic transformation into flat, enucleated squames. At the crux of this transformation are intracellular keratohyalin granules (KGs) that suddenly disappear as terminally differentiating KCs transition to the cornified skin surface. Defects in KGs have long been linked to skin barrier disorders. Through the biophysical lens of liquid-liquid phase separation (LLPS), these enigmatic KGs recently emerged as liquid-like membraneless organelles whose assembly and subsequent pH-triggered disassembly drive squame formation. To stimulate future efforts toward cracking the complex process of skin barrier formation, in this review, we integrate the key concepts and foundational work spanning the fields of LLPS and epidermal biology. We review the current progress in the skin and discuss implications in the broader context of membraneless organelles across stratifying epithelia. The discovery of environmentally sensitive LLPS dynamics in the skin points to new avenues for dissecting the skin barrier and for addressing skin barrier disorders. We argue that skin and its appendages offer outstanding models to uncover LLPS-driven mechanisms in tissue biology.

JID Innovations (2021);**1:**100036 doi:10.1016/j.xjidi.2021.100036

Toward cracking the skin barrier

Skin is the largest and foremost defensive and sensory organ in the human body (Pasparakis et al., 2014). At the interface with the external environment, the epidermal surface seals the skin as a tight and environmentally responsive tissue barrier. Essential to life, this mammalian skin barrier prevents water loss, excludes pathogens, and provides resistance to physical and chemical insults (Madison, 2003).

The architecture and cellular dynamics of the epidermis are key to its protective barrier function. The epidermis is a stratified squamous epithelium in which transcriptionally active keratinocytes (KCs) constantly flux upward toward the skin surface. Self-renewal begins at the innermost basal layer of the epidermis, where epidermal stem cells divide and fuel terminal differentiation. Along their upward differentiation path, KCs acquire defining structural features demarcating three distinct stages: the spinous, granular, and corneum layers (Fuchs, 2007; Moreci and Lechler, 2020). Under tissue homeostasis, mouse KCs flux from the basal to the granular layer with stereotypical transit times, but they proceed stochastically through the granular-to-corneum transition (Rompolas et al., 2016). The granular layer appears to act as a buffer zone with yet unknown mechanisms to coordinate the formation of cornified tissue (Rompolas et al., 2016; Yokouchi et al., 2016). When KCs in the granular layer reside at the corneum interface, they abruptly transform into corneocytes by losing their nuclei and cytoplasmic organelles (Eckhart et al., 2013). This KC-to-corneocyte transition is critical: corneocytes with squame features pile tightly, depositing and maturing intercorneocyte lipid structures that are key to the skin's permeability barrier (Narangifard et al., 2021; Winsor and Burch, 1944). Because surface corneocytes are sloughed off in response to persistent environmental pressures, the underlying layers replenish the corneum to sustain barrier integrity (Kubo et al., 2012; Rompolas et al., 2016; Rübsam et al., 2017; Yokouchi et al., 2016). This epidermal turnover in human skin is robust, estimated at about 3.7 billion cells per day—about 1% of the total daily cellular turnover in humans (Sender and Milo, 2021).

The epidermal dynamics underlying cellular turnover in the skin are sensitive to environmental demands and shift dramatically on instances of barrier disruption and skin inflammation. Yet, the cellular mechanisms that couple epidermal differentiation and environmental pressures on the skin barrier remain largely unknown. Mounting evidence points to the granular layer as crucial to the formation of a functional and environmentally resilient cornified layer. For example, an immature or absent granular layer is strongly linked to human disorders involving abnormal cornification and dysfunctional skin barrier phenotypes exacerbated by environmental extremes (Kantor and Silverberg, 2017; Mlitz et al., 2012; Palmer et al., 2006; Smith et al., 2006; Thyssen et al., 2020). These differentiation defects literally crack the barrier, offering mechanistic clues (Martins et al., 2018) to figuratively crack the mechanisms underlying skin barrier formation.

To unravel the epidermal dynamics and environmental responsiveness of the skin barrier in health and disease, we

[1]*Wallace H. Coulter Department of Biomedical Engineering, Georgia Institute of Technology and Emory University, Atlanta, Georgia, USA*

Correspondence: Felipe Garcia Quiroz, Wallace H. Coulter Department of Biomedical Engineering, Emory University, Atlanta, Georgia 30322, USA. E-mail: felipe.quiroz@emory.edu

Abbreviations: 3D, three-dimensional; AD, atopic dermatitis; CE, cornified envelope; EDC, epidermal differentiation complex; ER, endoplasmic reticulum; IDP, intrinsically-disordered protein; KC, keratinocyte; KG, keratohyalin granule; LCST, lower critical solution temperature; LLPS, liquid-liquid phase separation; PTM, post-translational modification; TG, trichohyalin granule; UCST, upper critical solution temperature

Received 27 March 2021; revised 7 June 2021; accepted 18 June 2021; accepted manuscript published online 6 July 2021; corrected proof published online 3 September 2021

Cite this article as: JID Innovations 2021;1:100036

argue that the granular-to-corneum transition will require dissection at the tissue, cellular, and subcellular levels. Historically, tackling this challenge faced steep technical and conceptual barriers that prevented progress. Prominent among these barriers, we lacked biophysical tools and frameworks to predict, chart, and visualize the behavior of key proteins and cellular processes involved in this rapid and complex differentiation program. With recent progress toward addressing these gaps, as we will explain, the scientific landscape is ripe to crack enigmatic cellular mechanisms that underlie skin barrier formation.

A subset of key proteins throughout epidermal differentiation are intrinsically-disordered proteins (IDPs) that defy the traditional interpretation of proteins as ordered molecular solids (Figure 1a). Long underappreciated in protein biology, IDPs recently emerged as major drivers of intracellular self-assembly. We and others have begun to chart their unique sequence-encoded properties in cells and across biological systems (Quiroz and Chilkoti, 2015; Wang et al., 2018), including skin (Quiroz et al., 2020). Furthermore, epidermal cells that flux through the granular layer are typified by the emergence and loss of poorly understood IDP-rich, membraneless protein granules. These dynamic cytoplasmic structures, which have counterparts across cornifying epithelia, have been notoriously difficult to study. Excitingly, new tools and concepts from the multidisciplinary field of liquid-liquid phase separation (LLPS) now enable us to approach membraneless protein granules as functional and highly dynamic organelles (Bergeron-Sandoval et al., 2016; Shin and Brangwynne, 2017). Building on these insights, we recently exposed keratohyalin granules (KGs), the protein granules of granular layer cells, as liquid-like membraneless organelles whose assembly and disassembly fuel skin barrier formation (Quiroz et al., 2020).

In this review, we integrate concepts, tools, and approaches spanning IDP research, LLPS, and skin biology as a step toward cracking the process of skin barrier formation. We expect that discussion of the biophysical frameworks and recent findings in the skin will equip biologists and clinicians with an LLPS-inspired lens to study the skin barrier. Using this lens, we illuminate new hypotheses at the interface of novel and known cellular mechanisms at play in barrier formation. As a corollary, for readers with a multidisciplinary background, this review exposes skin and its appendages as fascinating tissue and organ systems to examine LLPS-driven mechanisms.

Phase separation-driven assembly of membraneless organelles

How are cellular compartments that are not bound by lipid membranes, such as KGs in the skin, stabilized to function as organelles? How do they achieve selective component exchange with their surroundings? Mechanistically, how do their structural and molecular features contribute to cellular processes? Over the last decade, answers to these questions have emerged from the biophysical framework of LLPS (Banani et al., 2017; Quiroz et al., 2020). Fueled by thought-provoking observations of liquid-like behavior in germline-defining granules (Brangwynne et al., 2009), combined with progress on the sequence encoding of LLPS in IDPs (Dzuricky et al., 2018; Quiroz and Chilkoti, 2015; Wang et al., 2018), the stage is set to dissect the physiological roles of long-overlooked membraneless compartments in stratifying epithelia and across biological systems.

Membraneless structures have long puzzled biologists. In the 1830s, the highly refractive nucleolus, visible through brightfield microscopy, emerged as the first documented intranuclear compartment (Trinkle-Mulcahy, 2018). By the late 1890s, the use of fixatives and dyes exposed cytoplasmic granules linked to epidermal differentiation (Holbrook, 1989) and to germline specification (Hegner, 1911, 1908). Additional biochemical methods revealed now-stereotypical membraneless organelles of the nucleus: Cajal bodies (Cajal, 1903) and speckles (Cajal, 1910; Gall, 2003; Lamond and Spector, 2003). Crucially, beginning in the 1940s, high-resolution electron microscopy confirmed the membraneless nature of nucleoli (Leblond, 1981; Trinkle-Mulcahy, 2018) and of other intracellular granules, including KGs (Lavker and Matoltsy, 1971) and germline-defining granules (Mahowald, 1962). Later in the 1980s, benefiting from immunofluorescence, Strome and Wood (1982) documented the germline granules of *Caenorhabditis Elegans*, coining the term P granules. Despite this progress, imaging fixed cells reinforced the view of membraneless structures as solid granules rather than viscous liquids. This issue was presciently described by Wilson (1899), who noted the liquid or viscous structures of living starfish oocytes under pressure, positing that (without fixation) intracellular granules and other spherical protoplasmic bodies behaved as a fine emulsion.

The driving forces behind the assembly and dynamics of membraneless organelles remained largely unexplored for decades. These mechanistic underpinnings came to the forefront in 2009 when the seminal work by Brangwynne et al. (2009) established that the formation and material properties of P granules were grounded in LLPS dynamics (Figure 1b–d). They showed that P granules formed in a concentration-dependent manner and exhibited classic liquid-like behaviors of flow under shear stress and rapid fusion into larger droplets (Figure 1c). Building on these observations, they linked P granule assembly to the physics of phase transition polymers, which undergo demixing phase separation to form polymer-rich phases (LLPS condensates) in aqueous solutions. The resulting cross-disciplinary bridge, linking the theoretical framework of LLPS to a broad range of ribonucleoprotein granules, led to a general framework to describe the formation and dynamics (assembly/disassembly, growth, viscosity, buffering capacity) of membraneless organelles (Banani et al., 2017; Jawerth et al., 2020; Klosin et al., 2020). Subsequent work with nucleoli (Brangwynne et al., 2011), other ribonucleoprotein assemblies (Garcia-Jove Navarro et al., 2019; Sawyer et al., 2019), and model LLPS condensates (Kaur et al., 2021) have further delineated this link between LLPS and the liquid-like behaviors of membraneless organelles.

Over the last decade, a revolution unfolded in pursuit of a biomolecular understanding of LLPS. Going beyond the physicochemistry of synthetic polymers naturally prompted key questions: what biomacromolecules drive LLPS in cells? How is their LLPS controlled at cellular and molecular levels? Initial progress centered on the disordered and aggregation-

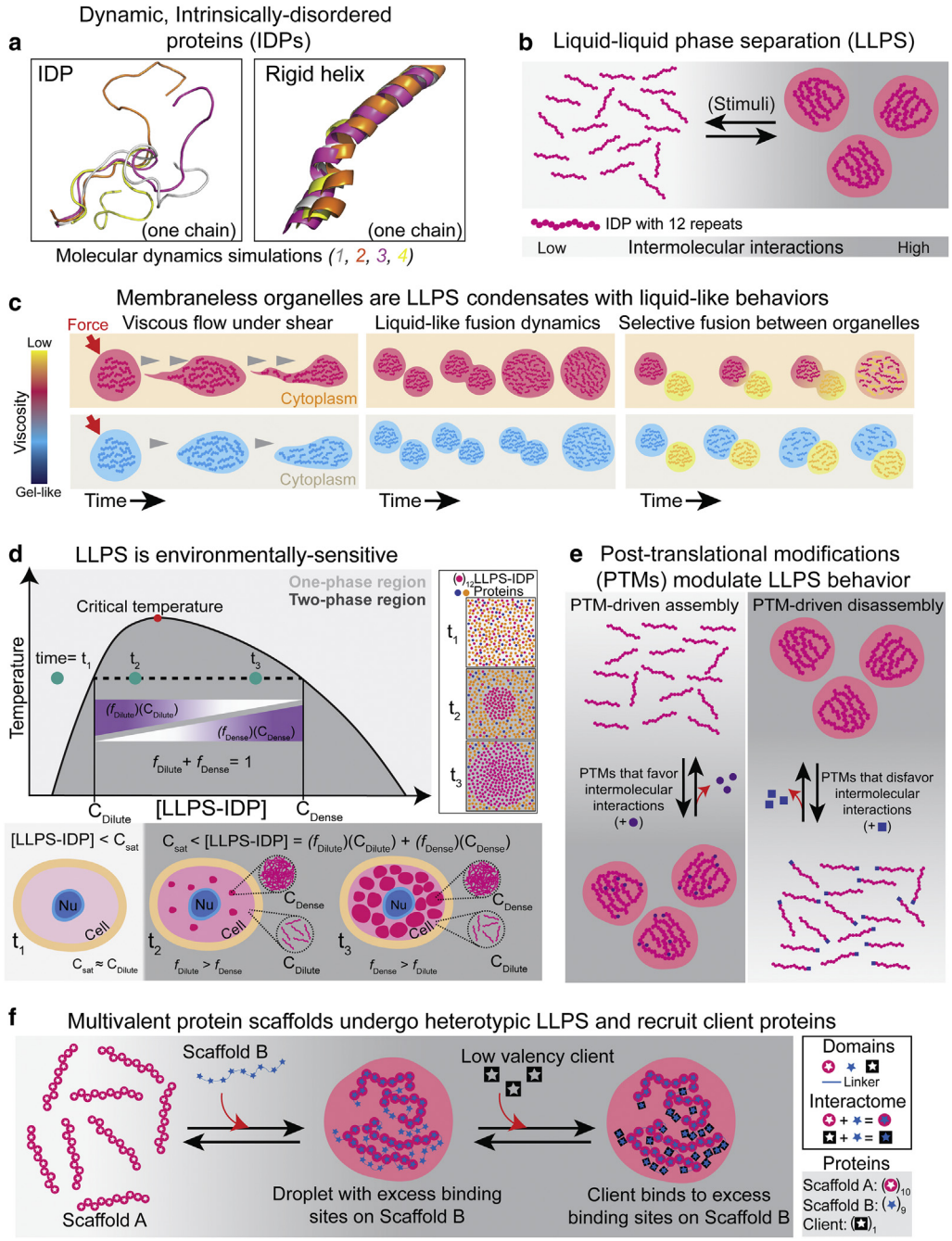

Figure 1. Phase separation-driven assembly of membraneless organelles. (**a**) IDPs exhibit dynamic structural fluctuations. In snapshots from four separate molecular dynamics simulations, a model IDP (left) fails to adopt a defined three-dimensional structure, whereas a helical protein domain (right) reproducibly folds into the same helical solid. Adapted from Quiroz and Chilkoti (2014). (**b**) Resistant to folding, IDPs engage in extensive intermolecular interactions. When these sequence-dependent and stimuli-sensitive interactions increase over a critical threshold, an LLPS transition ensues: a large fraction of IDP molecules coalesce into condensates. As a model LLPS-IDP, we consider an IDP with a repetitive architecture. Repeats are not essential for LLPS but are common in IDPs and readily tune their LLPS behavior (Quiroz and Chilkoti, 2015). (**c**) Membraneless organelles have properties akin to liquids such as (left to right) flow under shear force, rapid fusion between similar droplets, and selective fusion with dissimilar droplets. Intermolecular forces between scaffolds and/or LLPS-IDPs determine the viscosity and surface tension of these liquid-like organelles. Viscosity alters the speed of flow (gray arrows; left panel) and the kinetics of fusion events (middle panel). Less intuitively, the condensates assembled by distinct scaffolds or LLPS-IDPs are either miscible (top right panel) or immiscible (bottom right panel). The outcome of these organelle interactions ultimately depends on surface tension, surface charge, and the potential/affinity of cross-scaffold interactions (Kaur et al., 2021). (**d**) Representative phase diagram as a function of environmental stimuli (in this situation, temperature) and protein concentration for polymers and IDPs that exhibit UCST LLPS. Above a critical point (the UCST), irrespective of LLPS-IDP concentration ([LLPS-IDP]), the system resides in the one-phase region (light gray): low intermolecular interactions between LLPS-IDP chains are never conducive to LLPS. To illustrate LLPS under the UCST, we consider a cell actively synthesizing an LLPS-IDP at a constant temperature. At t_1, intracellular LLPS-IDP levels are below the C_{sat} or critical concentration for phase separation—equivalent to C_{Dilute} under equilibrium. Under these conditions, LLPS-IDP molecules are diffuse and are well-mixed with other proteins in the cytoplasm (t_1, bottom and right panels). On sustained protein synthesis, at t_2, intracellular LLPS-IDP concentration increases over C_{sat}, driving the system into the two-phase regime (dark gray). LLPS-IDP molecules now reside in one of the two phases: a condensate or high-density phase (at C_{Dense}) and a dilute phase (at C_{Dilute}). As a result, a fraction of LLPS-IDP molecules markedly demixed from other proteins in the cytoplasm (t_2, bottom and right panels). Moving along the tie line (dashed line) as intracellular LLPS evolves from t_2 to t_3, further increases in total LLPS-IDP levels do not alter C_{Dense} or C_{Dilute} but increase the

prone domains of RNA-binding proteins —for their enrichment in prominent ribonucleoprotein granules (Kato et al., 2012). Multidisciplinary efforts eventually converged on IDPs, multivalent protein scaffolds, and RNAs as key players that govern LLPS in the cell (Banani et al., 2017).

History aside, we turn to key concepts and extant biomolecular LLPS frameworks that illuminate our current understanding of membraneless organelles. First, consider IDPs. Once thought uncommon (Dunker et al., 2001), IDPs and proteins with IDP domains abound in eukaryotic proteomes (van der Lee et al., 2014). IDPs are akin to synthetic polymers, failing to adopt defined three-dimensional (3D) structures to hide away interaction-prone molecular features (Figure 1a) (van der Lee et al., 2014). The amino acid composition/sequence of each IDP and the intracellular milieu (solvent) ultimately determine the likelihood, means, and timing of their LLPS behavior. Paralleling observations in synthetic polymers, LLPS leading to condensate formation only occurs when the overall conditions favor intermolecular interactions over IDP-solvent interactions (Figure 1b). Yet, dissecting the intracellular LLPS of IDPs in vivo remains challenging (Alberti et al., 2019). The underlying challenge is two-fold: (i) IDPs span structural features and behaviors intermediate between synthetic polymers and folded proteins and (ii) lack of control/understanding of dynamic cell-specific variables that alter IDPs and their LLPS behavior.

Borrowing from polymer physics, the LLPS behavior of IDPs may be mapped onto phase diagrams wherein two key variables describe IDP demixing and condensate formation in cells (Figure 1c) (Brangwynne et al., 2015). The value of this approach relies on the assumption that despite the complexity of the intracellular environment, homotypic interactions dominate the LLPS behavior of a particular IDP. This assumption is reasonable for prototypical LLPS-exhibiting IDPs but may be inadequate for IDPs with LLPS-modifying intracellular binding partners (e.g., RNA for RNA-binding IDPs) and IDPs with low LLPS propensity. The latter may rely on heterotypic cooperation with other IDPs to drive intracellular LLPS (Riback et al., 2020). Phase diagrams for synthetic polymers and IDPs take on different shapes depending on the dominant molecular interactions. The phase diagram depicted in Figure 1c is typical of polymers that only undergo LLPS below an upper critical solution temperature (UCST)—picture the gelation of refrigerated gelatin. Some IDPs exhibit an inverted type of phase diagram defined by a lower critical solution temperature (LCST) (Ambadipudi et al., 2017; Quiroz and Chilkoti, 2015; Riback et al., 2017). Characterization of intracellular LLPS has primarily focused on the UCST-type behavior exhibited by oft-studied RNA-binding IDPs (Bracha et al., 2018; Nott et al., 2015), but IDPs with LCST behavior are well-known from studies of elastin (Brangwynne et al., 2015; Dzuricky et al., 2018; Urry et al., 1974, 1969).

LLPS-exhibiting IDPs are enriched in low complexity and repetitive amino acid motifs that engage in multivalent and weakly adhesive interactions (Alberti et al., 2019; Brangwynne et al., 2015; Kato et al., 2012). Whether an IDP exhibits LCST or UCST LLPS is specified at the compositional amino acid level, with the molecular features of specific residues influencing the nature of peptide–peptide interactions (Dignon et al., 2019; Quiroz and Chilkoti, 2015; Wang et al., 2018). These LLPS-specific interactions involve combinations of charge–charge, cation–pi, pi–pi, hydrogen-bonding, and hydrophobic contacts (Das et al., 2020; Quiroz and Chilkoti, 2015). Whereas LCST IDPs favor hydrophobic interactions involving aliphatic residues, UCST IDPs often rely on cation–pi and pi–pi interactions involving aromatic and arginine residues. Beyond compositional bias, IDPs are sequence-controlled polymers wherein subtle changes at the sequence level potently shift LLPS dynamics (Quiroz et al., 2019). Although poorly understood, sequence-encoded behaviors set IDPs apart from synthetic polymers. These observations suggest that some membraneless organelles may access unique types of nonequilibrium LLPS dynamics (Jawerth et al., 2020; Quiroz et al., 2019).

To intuit the value of temperature-dependent (UCST and LCST) LLPS frameworks in biological systems, consider that temperature is simply a dial of the underlying interaction energies. Changes in pH, ionic strength, and other environmental signals are common dials that either amplify or suppress LLPS, thus shifting the boundaries of the two-phase regime in the relevant phase diagram. Analogously, cells harbor sophisticated molecular dials to tune intermolecular IDP interactions. One major dial involves post-translational modifications (PTMs). Of note, IDPs and disordered protein segments are hotspots for PTMs in eukaryotic cells (Wright and Dyson, 2015). As shown in Figure 1e, PTMs such as phosphorylation potently alter the LLPS behavior of IDPs (Owen and Shewmaker, 2019; Pattanaik et al., 1991). The outcome of these PTMs depends on the molecular features of the PTM and the proteins and the IDPs involved, resulting in either assembly or disassembly of LLPS condensates (Wang et al., 2014). For example, in epidermal differentiation, we suspect that IDP phosphorylation plays a role in KG disassembly. Another dial of intracellular LLPS involves RNAs, which alter LLPS behavior upon interaction with RNA-binding IDPs (Garcia-Jove Navarro et al., 2019; Kaur et al., 2021; Langdon et al., 2018). This is the likely major role for RNAs in tuning intracellular LLPS, although some RNA sequences are themselves prone to LLPS (Jain and Vale, 2017). Temperature may also directly dial the LLPS behavior of IDPs in cellular contexts subject to environmental extremes. We will discuss this idea for LLPS

volume fraction of the condensate phase (f_{Dense}) at the expense of the dilute phase (f_{Dilute}). The progressive shift toward $f_{Dense} > f_{Dilute}$ (purple gradients) involves increases in the number and/or size of LLPS condensates (t_3, bottom and right panels). (**e**) PTMs may alter intermolecular interactions to either favor (left) or oppose (right) intracellular LLPS. (**f**) Model of multicomponent condensate assembly by multivalent scaffolds and low-valency clients. Heterotypic interactions between domains in multivalent scaffolds can lead to LLPS (Li et al., 2012), even if the scaffold proteins are incapable of exhibiting LLPS on their own. These systems inevitably follow complex phase diagrams that are not captured by the single-component LLPS-IDP system in **d**. Clients are readily enriched in these LLPS condensates by binding to sites on the multivalent scaffold. The identity of these clients contributes to the varied functionality of membraneless organelles (Banani et al., 2016). C_{sat}, saturation concentration; IDP, intrinsically-disordered protein; LLPS, liquid-liquid phase separation; LLPS-IDP, liquid-liquid phase separation–exhibiting IDP; Nu, nucleus; PTM, post-translational modification; UCST, upper critical solution temperature.

condensates near the skin surface, but related mechanisms may be at play in other barrier tissues. Temperature fluctuations are also intuitive dials for the LLPS dynamics linked to heat shock responses (Riback et al., 2017) and for biomolecular LLPS in poikilotherms.

Although the previously introduced biomolecular framework is IDP-centric, valency alone is a major determinant of intracellular LLPS (Banani et al., 2017; Sanders et al., 2020). In pioneering work by Li et al. (2012) and Banani et al., 2016, Rosen and his team expanded notions of biomolecular LLPS to include networks of interacting multivalent proteins. These studies showed that signaling proteins, which often feature folded repeat domains with small linker IDP segments, engage in heterotypic, multivalent interdomain interactions capable of driving LLPS. Similar to multivalent interactions in IDPs, these domain interactions are weak (low affinity) and are governed by PTMs. However, unlike self-interacting IDPs, PTMs on one multivalent protein alter its binding affinity to domains on other proteins in the network. Because these multivalent repeat proteins often localize to the cell membrane, these studies also uncovered intracellular two-dimensional LLPS condensates—rather than 3D spherical droplets—that stretch abutting the membrane surface (Su et al., 2016).

The expanded biomolecular understanding of LLPS has matured into a useful framework in which membraneless organelles are functionally and compositionally dissected into scaffolds and clients (Banani et al., 2017). Scaffolds are IDP or multivalent proteins, perhaps even RNAs, which drive intracellular LLPS to form biomolecular condensates. Clients may lack LLPS behavior of their own but accumulate within condensates through client-scaffold interactions. Although these interactions are commonly engineered and conceived as traditional lock-and-key models involving domains in clients and scaffolds (as shown in Figure 1f), the concept extends to ultraweak interactions between IDP scaffolds and IDP clients (Quiroz et al., 2020). However, this useful division of labor between clients and scaffolds should not distract from the possibility that their roles intertwine. Across the wide spectrum of potential intracellular clients (van der Lee et al., 2014), some client proteins may conditionally exhibit LLPS or modulate the LLPS dynamics of scaffolds and their membraneless organelles (Quiroz et al., 2020; Riback et al., 2020).

The diversity of mechanisms to encode and control biomolecular LLPS poses a major challenge to predict and study LLPS scaffolds and LLPS clients in the cell. However, this challenge represents an exciting research frontier (Hardenberg et al., 2020). Experimentally, elucidating the evolving material properties and heterogeneous composition of intracellular LLPS condensates remain key areas for progress. Although the integrity of LLPS condensates is typically compromised on tissue and cell lysis, preventing traditional purification, the advent of proximity-dependent proteomics promises to expose the biomolecular composition of membraneless organelles (Bracha et al., 2019; Markmiller et al., 2018; Yang et al., 2020). These approaches, coupled with emergent tools to probe in vivo LLPS without molecular tagging of IDP scaffolds (Quiroz et al., 2020), will fuel progress toward translating the LLPS-imparted dynamics of membraneless organelles into molecular mechanisms in cells and tissues (Dodson and Kennedy, 2020).

Membraneless organelles across stratifying epithelia

Despite the exciting progress in the field of LLPS-driven cellular mechanisms, we still know surprisingly little about the contribution of membraneless organelles and their LLPS dynamics to mammalian and tissue biology. This gap is at full display for abundant membraneless structures in the skin, namely the KGs of the epidermis and the trichohyalin granules (TGs) of hair follicles (Figure 2).

KGs are the subcellular structures that typify differentiating epidermal cells in the granular layer (Brody, 1977), disappearing as granular cells flux upward to the stratum corneum (Figure 2a). First visualized by Aufhammer in 1869 and confirmed as a hallmark of epidermal differentiation by Langerhans in 1873 (Matoltsy and Matoltsy, 1970), the enigmatic history of KGs mirrors that of other membraneless organelles (Holbrook, 1989). The term "keratohyalin granules," coined by Waldeyer in 1882, was inspired by their theorized role as the precursor to keratin—the intracellular substance of corneocytes—and their histological features reminiscent of proteinaceous hyalin (Matoltsy and Matoltsy, 1970). Initially misinterpreted as byproducts of mitochondrial and nuclear degradation or as aggregates of fragmented tonofibrils (an early name for keratin filaments) and even ribosomes, ultrastructural studies with radiolabeled amino acids ultimately established KGs as products of active protein synthesis. Crucially, these studies showed that KGs contained a histidine-rich protein, later identified as FLG (Figure 2b) (Fukuyama et al., 1965), and suggested that their growth involved granule fusion (Brody, 1959a). However, these early efforts often confused FLG-containing KGs with other membraneless structures of the mammalian epidermis, such as the cysteine-rich loricrin granules in rat epidermis (Fukuyama and Epstein, 1975; Holbrook, 1989; Matoltsy and Matoltsy, 1970). While we do not dwell on these pioneering efforts spanning over a century, their careful review (Holbrook, 1989) provides a fascinating window into scientific progress in skin and tissue biology.

The discovery of FLG as a major constituent of KGs propelled the field of epidermal biology. FLG proteins are large histidine-rich IDPs with a repetitive architecture (Figure 2b), which undergo extensive and species-specific processing throughout epidermal differentiation. We use FLG to refer to the full-length protein encoded by the repetitive gene *FLG*, irrespective of mammalian species. The goal is to avoid confusion with the historical use of the term filaggrin, which specifically refers to a small basic protein that Dale (1977) isolated from the corneum of rat epidermis. Later shown to aggregate with purified keratin filaments (Dale et al., 1978), the underlying histidine-rich protein was eventually linked to a phosphorylated and oligomerized precursor from rat KGs (Lonsdale-Eccles et al., 1980). Steinert et al. (1981) subsequently proposed the name filaggrin to describe compositionally conserved small cationic proteins from the corneum of the mammalian epidermis, which they functionally defined by their ability to aggregate purified keratin filaments (Steinert et al., 1981). When subsequent work established the repetitive rather than oligomerized nature of the unprocessed filaggrin precursor, the term profilaggrin

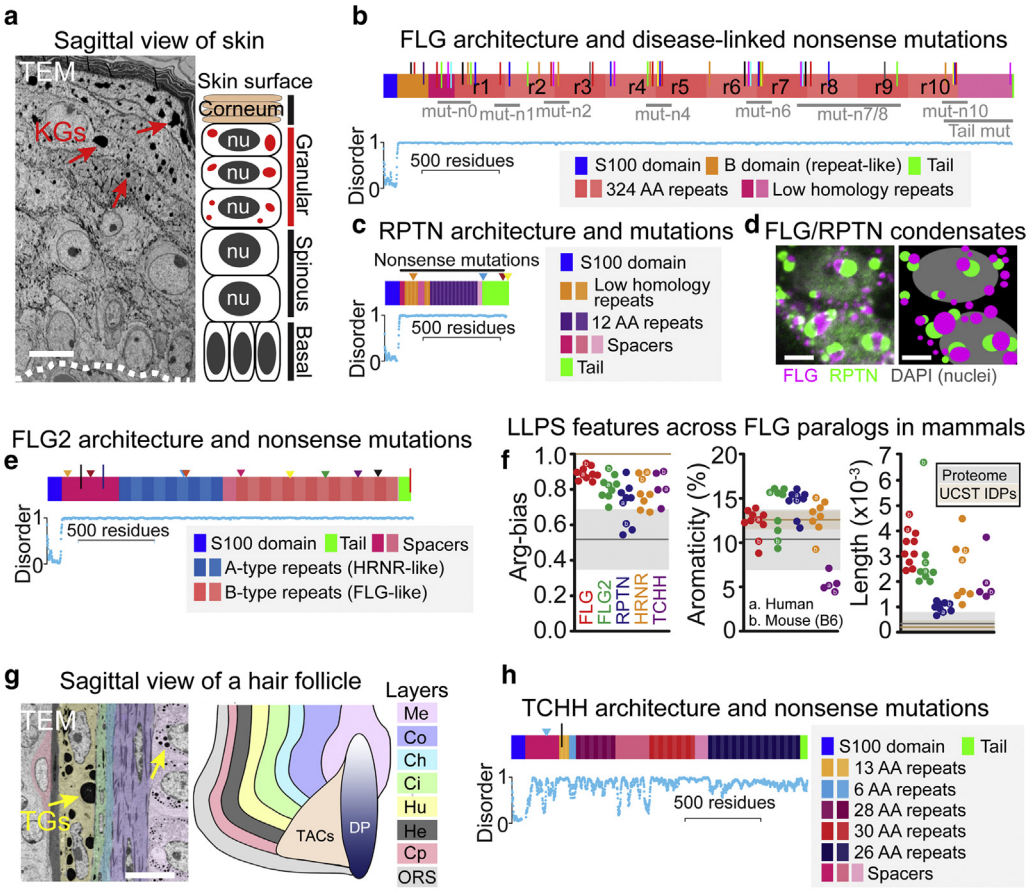

Figure 2. FLG and paralogs are IDPs that form membraneless organelles across stratifying epithelia. (**a**) Ultrastructure (TEM) and corresponding schematic of the mouse epidermis. Epidermal progenitor cells reside in the basal layer, attached to a basement membrane (dotted line). Progenitor cells flux upward to the skin surface, gaining KGs (red arrows) in the granular layer, which subsequently disappear as the cells move into the corneum. Adapted from Quiroz et al. (2020). Bar = 10 μm. (**b, c, e, h**) Domain architecture of human FLG, RPTN, FLG2, and TCHH and indicated location of disease-linked nonsense mutations (colored lines) as well as recurring nonsense mutations (>10 alleles) that await clinical interrogation (colored triangles) (Karczewski et al., 2020). Below the domain architecture, we show the disorder plots that predict the probability of IDP regions (Jones and Cozzetto, 2015). A value of 1 indicates disorder. FLG paralogs share a repetitive architecture with N-terminal S100 domains. These S100 domains have conserved hydrophobic pockets but distinct surface chemistries (Hinbest et al., 2020). (**b**) Mutations in the repeat domain of *FLG* (labeled as clusters: mut-n0 to mut-n10) generate truncated FLG variants that are strongly associated with atopic dermatitis; adapted from Quiroz et al. (2020). (**d**) FLG (pink) and RPTN (green) form distinct immiscible condensates when HaCATs differentiate and stratify at the air–liquid interface; adapted from Quiroz et al. (2020). Bar = 5 μm. (**e**) FLG2 has two domains that exhibit repeat architecture. The A-type repeat domain resembles HRNR repeats, whereas the B-type domain resembles FLG repeats (Wu et al., 2009a). Truncating mutants of FLG2 are associated with atopic dermatitis in African Americans (Margolis et al., 2014) and with Peeling Skin Syndrome (Alfares et al., 2017; Mohamad et al., 2018). (**f**) Analysis of FLG and paralogs in mice, humans, and other mammalian species show that FLG family proteins have conserved sequence features that encode for UCST-type LLPS in IDPs. Adapted from Quiroz et al. (2020); see the supplementary materials in the study by Quiroz et al. (2020) for a complete list of the studied mammalian species. (**g**) Ultrastructure (left) and schematic (right) of the organization of a mouse hair follicle. The hair follicle layers are depicted from the deepest to most superficial layers: Me, Co, Ch, Ci, Hu, He, Cp, and ORS. TEM image is courtesy of H. Amalia Pasolli and Elaine Fuchs at Rockefeller University (New York, NY); layer annotations were performed by H. Amalia Pasolli. Schematic of hair follicle layers was adapted from Yang et al. (2017). Bar = 10 μm. (**h**) TCHH displays a repetitive architecture with five repeat families. This sequence diversity contributes to a ragged disorder profile, in which low-disorder segments are prone to α-helical conformations (Lee et al., 1993). A nonsense mutation at residue 331 is associated with Uncombable Hair Syndrome (Ü Basmanav et al., 2016). AA, amino acid; Arg, arginine; DP, dermal papilla; IDP, intrinsically-disordered protein; KG, keratohyalin granule; LLPS, liquid-liquid phase separation; nu, nucleus; TAC, transit-amplifying cell; TCHH, trichohyalin; TEM, transmission electron microscopy; TG, trichohyalin granule; UCST, upper critical solution temperature; Me, medulla; Co, cortex; Ch, hair shaft cuticle; Ci, inner root sheath cuticle; Hu, Huxley's layer; He, Henle's layer; Cp, companion layer; ORS, outer root sheath.

was adopted (Harding and Scott, 1983), influencing the pioneering characterization of the human *FLG* gene (Presland et al., 1992). However, the modern descriptions of this gene (*FLG*) (Brown and McLean, 2012) and protein (FLG) do not attempt to capture how filaggrin led to the discovery of profilaggrin. We adopt and recommend this simplification because the suggested nomenclature adequately shifts focus from specific roles of FLG processing byproducts to the overall functionality of FLG and its KGs.

The subtle shift from filaggrin to FLG becomes relevant to approach the poorly understood relationships between KG formation/loss and FLG synthesis/processing in skin barrier formation. For example, besides a repeat IDP domain, FLG features an N-terminal calcium-binding and dimerizing S100 domain (Presland et al., 1997). Long known to be cleaved during epidermal differentiation (Hinbest et al., 2020; Presland et al., 1992), the exact role and fate of this S100 domain remain unclear. Arguably, the only firmly established role of in vivo FLG processing is to provide the prime source

of UV-protecting and water-binding free amino acids and amino acid derivatives that keep corneocytes hydrated (Scott and Harding, 1986; Scott et al., 1982). Adding to the environmental sensitivity of the skin barrier, this breakdown of FLG fragments in the corneum occurs in a humidity-dependent manner (Scott and Harding, 1986). Low humidity promotes the deimination of FLG fragments (Cau et al., 2017), which accelerates their degradation by Caspase-14 (Denecker et al., 2007; Hoste et al., 2011) and bleomycin hydrolase (Kamata et al., 2009). Disruption of complete FLG processing compromises the hydration and mechanical properties of corneocytes (Thyssen et al., 2020). Several additional proteases contribute to the early stages of FLG processing, including SASPase (ASPRV1) (Matsui et al., 2011), matriptase (ST14) (Alef et al., 2009; List et al., 2003), and prostasin (PRSS8) (Leyvraz et al., 2005; Netzel-Arnett et al., 2006). However, all the steps before complete FLG degradation, including details of how FLG fragments interact with keratin filaments in the corneum, are incompletely linked to barrier function. For example, disruption of SASPase alters early FLG cleavage products but does not compromise FLG processing to free amino acids, inexplicably reducing corneum hydration and corneocyte stiffness (Matsui et al., 2011; Thyssen et al., 2020). As we will explain, dissecting the overall functionality of FLG and the cellular mechanisms involving its KGs will be key to continued progress in skin barrier research.

Centuries-old observations linking the absence of KGs to skin pathology (Brody, 1977; Harding and Scott, 1983) continue to fuel fascination with the functional significance of KGs. Although the pioneering work by Unna focused on psoriatic skin (Brody, 1977), the first molecular links to a defect in FLG synthesis came from families affected by ichthyosis vulgaris (Sybert et al., 1985). The latter is the most common inherited disorder of epidermal differentiation, marked by varying degrees of dry and rough skin (Brown and McLean, 2012). Yet, the challenge of sequencing the highly repetitive *FLG* gene long delayed the efforts to uncover the genetic basis of this autosomal semidominant skin disorder (Brown and McLean, 2012). Beginning in 2006, refined genotyping strategies firmly established that FLG truncations, namely p.R501X and c.2282del4, cause ichthyosis vulgaris (Smith et al., 2006). These two nonsense mutations, which account for >80% of the *FLG* loss-of-function mutations in Northern Europeans, and others spanning the FLG repeat domain (Figure 2b) are the strongest risk factor for atopic dermatitis (AD) (Palmer et al., 2006; Sandilands et al., 2007; Wong et al., 2018). Highly prevalent among patients with ichthyosis vulgaris and strongly associated with allergies, AD is a common skin inflammatory disorder, a type of eczema in which dry and rough skin may get severely itchy. The *FLG* mutational landscape varies substantially with ethnicity (Chen et al., 2008; Nomura et al., 2007; Palmer et al., 2006; Zhu et al., 2021). FLG also exhibits intragenic copy (repeat) number variation (between 10 and 12 repeats), and the largest variants are associated with a reduced risk of suffering from skin barrier disorders (Brown et al., 2012; Margolis et al., 2020a).

The refined understanding of KGs and FLG was intimately linked to progress in identifying the epidermal differentiation complex (EDC) (Mischke et al., 1996), a gene cluster in human chromosome 1 that governs terminal differentiation (de Guzman Strong et al., 2010; Moreci and Lechler, 2020). Probing the EDC led to the identification of novel FLG paralogs with an S100-fused type architecture, namely RPTN (Krieg et al., 1997), HRNR (Makino et al., 2001), CRNN, and most recently FLG2 (Wu et al., 2009a). These FLG paralogs remain understudied without consensus on their tissue specificity, processing, abundance, and functional significance. Except for the unusually small CRNN, their localization is linked to epidermal KGs (Huber et al., 2005; Wu et al., 2009a, 2009b). These reports hint at the heterogenous composition of KGs, but the evidence remains scarce. RPTN, for example, features a prominent IDP domain (Figure 2c) and can form distinct membraneless granules that interact with FLG-containing KGs (Figure 2d) (Quiroz et al., 2020). FLG2 features a long IDP domain with FLG-like repeats (Figure 2e) and is closest to FLG in aspects of in vivo processing and epidermal expression (Hsu et al., 2011; Pendaries et al., 2015). FLG2 is also generally believed to colocalize with FLG in KGs (Hsu et al., 2011; Wu et al., 2009a). Although heterozygous FLG2 truncations are linked to the persistence of AD in African Americans (Margolis et al., 2014), FLG and FLG2 may serve nonoverlapping roles in skin barrier formation (Mohamad et al., 2018). For example, homozygous FLG2 truncations are uniquely linked to a skin peeling syndrome (Alfares et al., 2017; Mohamad et al., 2018). Unlike FLG, FLG2 shows appreciable localization to the cornified envelope (CE), a hallmark protein-reinforced plasma membrane of corneocytes (Albérola et al., 2019). Notably, FLG fragments are often cited as contributing to the CE, despite evidence that very small amounts of FLG fragments localize to the CE (Manabe et al., 1991; Simon et al., 1996; Yoneda et al., 1992). The significant variance in sequence and architecture across FLG and FLG paralogs suggest specialized roles in epidermal biology, but their association with KGs or distinct membraneless condensates likely influences their functionality. One striking observation that insinuates functional LLPS capabilities is that FLG and its paralogs all share key compositional determinants of UCST-type behavior (Figure 2f) (Quiroz and Chilkoti, 2015; Quiroz et al., 2020).

Soon after the early studies of KGs in the epidermis, the hyalin of the hair drew intense interest. In 1903, Voerner first reported TGs in cells of the inner root sheath and medulla layers of hair (Figure 2g) (Hamilton et al., 1991). Reminiscent of KG dynamics, the formation of subcellular TGs hallmarks distinct stages of hair follicle differentiation, disappearing abruptly as cells undergo terminal differentiation (Birbeck and Mercer, 1957; O'Keefe et al., 1993). Similar to KGs, TGs exist in close association with keratin filaments, and their formation and processing are convincingly yet incompletely linked to the high-order structuring of the keratin network (O'Guin et al., 1992). Some early descriptions of TG dynamics suggested that they behaved as viscous insoluble liquids, coalescing to form larger droplets before their sudden disappearance (Birbeck and Mercer, 1957). The major known protein component of TGs is TCHH, a large IDP-like protein (Figure 2h) first isolated from wool follicles (Rothnagel and Rogers, 1986). Similar to *FLG*, the *TCHH* gene was a founding member of the EDC complex (Mischke et al., 1996)

and features an FLG-like repetitive architecture (Lee et al., 1993). Apart from having an S100 domain fused with a long repetitive segment, the amino acid sequence and composition of TCHH are strikingly different from those of FLG (Lee et al., 1993; Rothnagel and Rogers, 1986). Figure 2h shows the ragged disorder profile of TCHH, with some repeat segments having a high alpha-helical propensity (Lee et al., 1993). TCHH is one of the most enriched in charged residues across the human proteome (Lee et al., 1993), with arginine and glutamine accounting for nearly 50% of its composition. TCHH has long been shown to undergo extensive citrullination (Rogers, 1964; Rothnagel and Rogers, 1986), which has been implicated in TG dissolution and transglutaminase-mediated crosslinking of TCHH with itself and with keratins (Tarcsa et al., 1997). These crosslinking events are considered the primary mechanism by which TCHH mechanically strengthens terminally differentiated inner root sheath cells (Steinert et al., 2003).

Beyond epidermal and hair differentiation, KGs and TGs recur in terminal differentiation programs across stratifying epithelia. TGs feature prominently in the filiform papillae of the tongue (O'Keefe et al., 1993), whereas KGs are abundant in the epithelium of the hard palate (De Benedetto et al., 2008; Smith and Dale, 1986). Similar to our observation of interacting KGs and RPTN granules (Figure 2d), immunogold labeling of tongue epithelium has revealed intriguing interactions between KGs and TGs (Manabe and O'Guin, 1994). A subset of cells in the granular layer of the human epidermis contain TGs (Hamilton et al., 1991), but their frequency and significance remain unexplored. However, as we explain next, how KGs and TGs contribute to terminal differentiation begs intense exploration.

Liquid-liquid phase separation dynamics through skin barrier formation

Understanding FLG proteins as prototypical LLPS-exhibiting IDP scaffolds redefined the formation and disappearance of KGs as barrier-defining LLPS dynamics (Quiroz et al., 2020). Using live imaging and genetically engineered mice with epidermal expression of phase-separation sensors, Quiroz et al. (2020) uncovered the FLG-dependent LLPS-driven assembly, maturation, and disassembly of KGs. Figure 3a summarizes our current understanding of in vivo LLPS dynamics through epidermal stratification, as epidermal cells flux into the granular layer and through the granule-to-corneum transition.

KGs in early granular-layer cells occasionally grow through liquid-like fusion events (Figure 3b). However, as KCs move upward toward the skin surface, they become crowded with increasingly viscous KGs that grow primarily without fusion (Figure 3c). Departing from the extensive liquid-like fusion of de novo assembled KGs in cultured KCs, abundant in vivo keratin-1/keratin-10 (K1/K10) fibers interact with FLG on the surface of native KGs to cage them, preventing KG fusion (Figure 3c) (Quiroz et al., 2020). Through electron microscopy, these keratin-caged KGs appear prominently on horizontal, en face sections of mouse epidermis (Usui et al., 2019). Furthermore, this restriction of KG fusion by K1/K10 fibers likely controls KG size, as suggested by enlarged KGs on genetic ablation of K10 in mice (Kumar et al., 2015). In humans with epidermolytic hyperkeratosis characterized by *KRT1* and *KRT10* mutations, K1/K10 aggregates severely disrupt the overall cytoplasmic organization and result in unusually large KGs (Ishida-Yamamoto et al., 1994). The emergent picture suggests that a tug-of-war between KGs and keratin fibers structures the cytoplasm en route to cornification.

Coinciding with the granular-to-corneum transition (the top-right granular cell in Figure 3a), KGs begin to disassemble (Figure 3c). This sudden shift in KG-phase dynamics is triggered by an abrupt drop in intracellular pH (Figure 3d). The pH responsiveness of KGs is rooted in the pH-sensitive LLPS behavior of FLG, which becomes protonated as the intracellular pH approaches the pk_a (~pH 6.1) of its abundant histidine residues (Quiroz et al., 2020). Although the skin surface has been long known to be acidic, suggesting an extracellular pH gradient across the corneum layer, live imaging of KG-residing phase-separation sensors and intracellular pH reporters uncovered a novel intracellular pH shift as an upstream regulator of the granular-to-corneum transition (Quiroz et al., 2020). In complementary intravital imaging, Matsui et al. (2021) showed that this critical and rapid intracellular acidification occurs downstream of a tightly regulated and sustained increase in intracellular calcium levels. Before KG disassembly, viscous KGs distort nuclei (Figure 3e) and possibly other membrane-bound organelles. These KG-induced nuclear deformations contrast with the wetting of nuclear surfaces by P granules (Wei et al., 2017), suggesting that KGs are biomolecular condensates with distinct mechanical/viscous properties.

Crucial to skin barrier formation, pH-triggered KG disassembly initiates enucleation (Figure 3f). Combined live imaging of phase-separation sensors, chromatin, and intracellular pH reporters in mouse skin showed that upon the abrupt intracellular acidification, the release of KG-residing client proteins precedes chromatin compaction, leading to enucleation and squame-like features (Quiroz et al., 2020). In the early stages of enucleation, KG disassembly and intracellular acidification may facilitate nuclear entry and activation of DNase1L2 (Fischer et al., 2017, 2007; Matsui et al., 2021), which resides in the endoplasmic reticulum (ER) (Fischer et al., 2011) and is unique among DNase I family members in its dual dependence on calcium and acidic pH (active at pH $\leq$6.4) (Shiokawa and Tanuma, 2001). Importantly, when manipulating intracellular acidification of the granular layer, pH-triggered chromatin compaction occurred in a KG-dependent manner (Quiroz et al., 2020). In granular layer cells genetically depleted of KGs, the process of enucleation lost its characteristic rapid progression, and intracellular acidification failed to trigger chromatin compaction (Quiroz et al., 2020). Adding to these findings in mice, Ipponjima et al. (2020), working with human skin equivalents, showed that loss of FLG and KGs drastically lengthened the rapid morphological transformations underlying the granular-to-corneum transition.

That the enigmatic granular-to-corneum transition entails a pH-triggered shift in epidermal LLPS dynamics provides new biomolecular insights to probe the long-known association between absence/atypical KGs and cornification defects in the human epidermis (Brody, 1977; Manabe et al., 1991). To guide progress, initial efforts should map the differentiation and pH-dependent molecular composition of KGs,

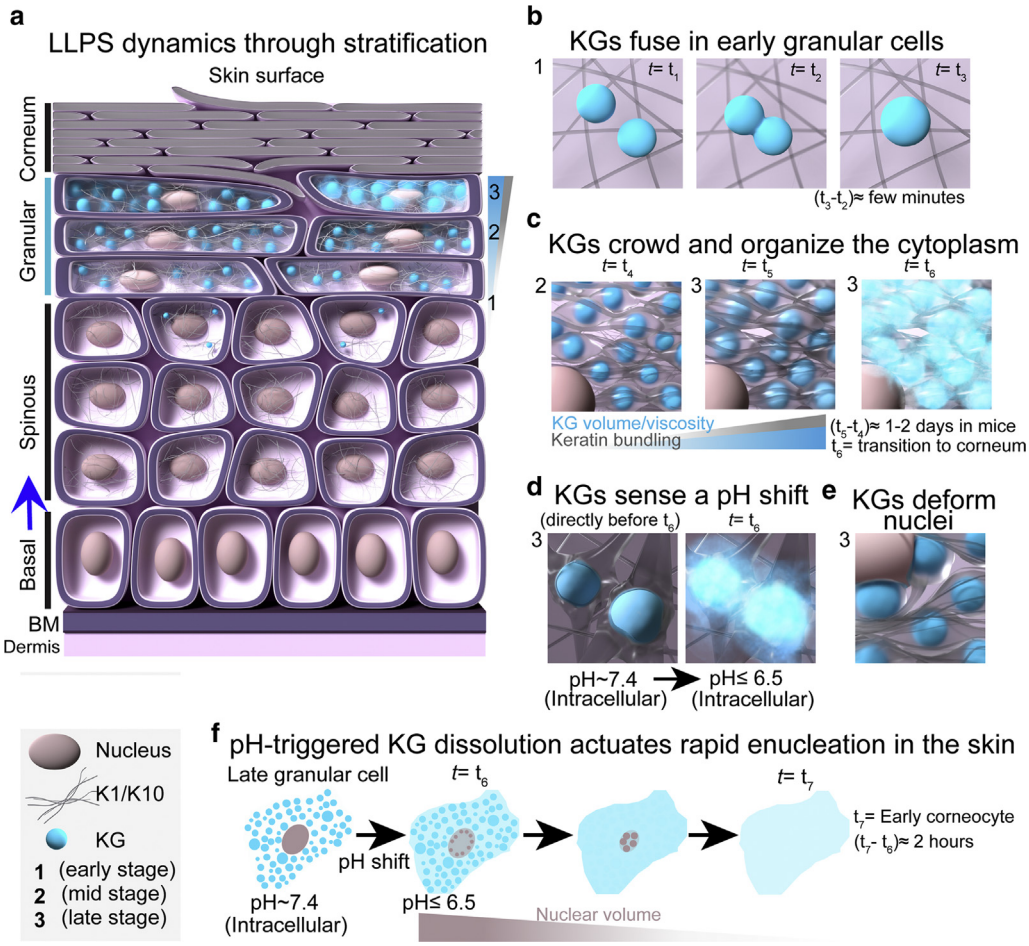

Figure 3. LLPS dynamics through epidermal stratification. (**a**) Shifting LLPS dynamics of KGs play a prominent role throughout epidermal stratification. On detachment from the BM, keratinocytes acquire keratin filaments formed by keratin-1/keratin-10 (K1/K10) heterodimers. Moving upward, keratinocytes upregulate *FLG*, triggering the LLPS-driven assembly of submicron KGs (stage 1), which later become prominently visible (≥1 μm in diameter) in the granular layer where FLG levels are highest. As cells move through the granular layer (stages 2 and 3), KGs grow in number and volume and become closely associated with keratin bundles as they crowd the cytoplasm. At the granular–corneum interface, one granular cell (top right) undergoes pH-triggered KG disassembly and nuclear compaction as it moves upward to the corneum. At the corneum layer, free of KGs, nuclei, and other organelles, corneocytes are filled with a highly ordered network of keratin filaments (Iwai et al., 2012). Under direct environmental stress, corneocytes at the skin surface eventually slough off, either cooperating with or responding to the underlying epidermal dynamics. The vertical gradient scales highlight the progressive crowding of the cytoplasm by KGs (cyan) and keratin bundles (gray). (**b–d**) Inspired by live imaging of KG-phase dynamics in mouse skin (Quiroz et al., 2020), these panels depict KG-phase dynamics inside a single keratinocyte as it fluxes through the granular layer (stages 1–3, time points t_1 through t_6). (**b**) In the early stages of KG assembly, KGs are not caged by keratin bundles (t_1), move freely, and exhibit liquid-like fusion events (t_2–t_3) that fuel their early growth. (**c**) As FLG levels rise and KGs become prominent (t_4), they are well-distributed in the cytoplasm, and keratin cages prevent their liquid-like fusion. With sustained FLG synthesis over the span of 1–2 days (t_4–t_5), KGs grow substantially in volume as FLG molecules flow from the dilute phase (cytoplasm) to the KG condensates. This KG growth is accompanied by an increase in their viscosity. As viscous KGs grow, keratin bundles and other organelles are compacted in the increasingly crowded cytoplasm. Suddenly (t_6), KGs begin to disassemble and release their contents to drive corneocyte formation. (**d**) KG-phase dynamics are pH sensitive. Immediately before cornification, the cell experiences an abrupt intracellular acidification that initiates KG disassembly. (**e**) In some mature granular layer cells (stage 3), viscous KGs prominently deform nuclei (Quiroz et al., 2020). When *FLG* truncation mutants do not abolish LLPS (e.g., mut-n8 and tail-mut in Figure 2b), these FLG mutants form less viscous KGs that wet the nuclear surface (Quiroz et al., 2020). (**f**) pH-triggered KG dissolution releases yet unknown KG components that actuate rapid enucleation, beginning with prominent chromatin compaction and quickly leading to organelle loss and squame features. BM, basement membrane; KG, keratohyalin granule; LLPS, liquid-liquid phase separation.

identifying KG clients that mediate enucleation/cornification and the enzymes involved in controlling KG disassembly. The latter is intriguing because given the high pH buffering capacity of large histidine-rich KGs, intracellular pH shifts are insufficient to complete KG disassembly. Nonetheless, intracellular acidification alters KG-phase dynamics, resulting in the partial release of FLG scaffold and prominent release of KG clients into the cytoplasm, while allowing entry of proteins previously excluded from KGs (Quiroz et al., 2020). To offer an example, in genetically engineered mice with epidermal expression of SEpHLuorin (a genetically encoded pH reporter), KGs exclude the pH reporter and only become enriched in SEpHLuorin upon the pH-triggered onset of KG disassembly—also revealing pH buffering inside of KGs (Quiroz et al., 2020). The underlying pH-triggered change in KG permeability likely exposes FLG scaffolds to PTMs, which further alter its LLPS behavior to favor KG disassembly.

Regarding PTMs of FLG, the prevailing notion is that FLG is rapidly phosphorylated on synthesis, before KG formation, and that FLG dephosphorylation occurs upstream of KG dissolution and FLG processing at the granular-to-corneum transition (Brown and McLean, 2012; Sandilands et al.,

2009). This widely held view is at odds with the discovery that LLPS-specific homotypic FLG–FLG interactions drive KG assembly. Considering epidermal LLPS dynamics, we suspect that the phosphorylation of FLG contributes to KG disassembly rather than to assembly. In line with this LLPS-inspired model, early attempts to transiently express FLG fragments in cultured cells showed that intracellular formation of KG-like structures does not involve FLG phosphorylation (Dale et al., 1997). Arguably, the current understanding of FLG as heavily phosphorylated has roots in the language barrier separating FLG and filaggrin. Whereas this purified FLG fragment appeared unphosphorylated in corneum extracts, larger FLG fragments from the granular layer appeared phosphorylated (Lonsdale-Eccles et al., 1982, 1980). When purified filaggrin was eventually linked to profilaggrin in KGs, phosphorylation was assigned to the earliest occurrence of detectable FLG before KG assembly (Lonsdale-Eccles et al., 1982, 1980). Complicating this context, subsequent characterization of FLG and FLG fragments relied on their pelleting from tissue lysates through dilution in ice-cold water—equivalent to IDP purification through thermally triggered LLPS (Quiroz and Chilkoti, 2015). Given the UCST-type LLPS behavior of FLG, this simple purification strategy likely skewed against phosphorylated FLG fragments (Resing et al., 1984), cementing the belief that phosphorylation is somehow specific to newly synthesized FLG. However, to our knowledge, we lack convincing evidence to link this phosphorylated precursor of filaggrin to KG-residing FLG in early granular-layer cells. Instead, we submit that the phosphorylated precursor derives from cells at the granular-to-corneum interface, where FLG phosphorylation may be at play in KG disassembly.

This LLPS-inspired model for phosphorylation-dependent KG disassembly has important implications. First, the model is consistent with observations that phosphorylation of FLG fragments prevents premature FLG-mediated keratin aggregation (Harding and Scott, 1983; Lonsdale-Eccles et al., 1982). Before KG disassembly, condensate-restricted FLG–keratin interactions occur and are beneficial to structuring the cytoplasm (Figure 3c). Second, the model is in line with recent phosphoproteomic data on UV-irradiated human skin equivalents (Yang et al., 2012). Third, the model invites the search for kinases capable of mediating FLG phosphorylation and KG disassembly at the granular-to-corneum transition. Finally, as originally suspected for rat FLG, subsequent proteolytic processing of FLG may occur in a phosphorylation-dependent manner (Resing et al., 1993). KG disassembly and FLG processing may also be modulated by intracellular acidification at the granule-to-corneum transition by SASPase (Matsui et al., 2021), which becomes active at pH $\leq$ 6.5 (Matsui et al., 2006).

Although several proteases contribute to processing FLG fragments to free amino acids, the early stages of FLG processing that are most relevant to shifting KG-phase dynamics remain poorly understood (Hoste et al., 2011; List et al., 2003; Matsui et al., 2011; Sandilands et al., 2009). Even the timing and role of the well-known cleavage of the N-terminal S100 domain of FLG remain unclear. However, this event has been typically assumed to occur at the granular-to-corneum transition, after KG dissolution (Cabanillas and Novak, 2016; Eckhart et al., 2013; Hoste et al., 2011; Sandilands et al., 2009). We recently learned that the S100 domain of FLG, which undergoes calcium-independent dimerization (Bunick et al., 2015), strongly promotes KG formation by reducing the critical concentration for intracellular LLPS of FLG (Quiroz et al., 2020)—equivalent to C_{Dilute} in Figure 1d. In engineered FLG proteins lacking S100 processing, the resulting intracellular KGs showed unusual stiffening, suggesting that early removal of the S100 domain may be required to sustain the liquid-like dynamics of KGs. Closing this knowledge gap, the composition of KGs in genetically engineered mice with epidermal expression of GFP fused to the S100 domain of mouse FLG (mS100-GFP) agrees with this early timing for S100 removal. In cultured KCs, the KGs assembled from unprocessed FLG prominently accumulate mS100-GFP, likely through S100-mediated dimerization. In contrast, native KGs in cells of the middle and late granular layers of mouse epidermis prominently excluded mS100-GFP (Quiroz et al., 2020). These in vivo data point to the removal of the S100 domain soon after KG assembly, with the S100 domain primarily facilitating KG formation. This model is consistent with reports showing that HRNR and extracted full-length FLG react poorly with antibodies directed to the S100 domain (Presland et al., 1997; Wu et al., 2009b).

Under the lens of LLPS, establishing KG-phase dynamics is a primary role for FLG. The axiom follows that *FLG* nonsense mutations must interfere with KG assembly and KG maturation. In line with this view, quantitative live-cell imaging of fluorescently tagged FLG mutants showed that truncation of the FLG repeat domain potently alters the critical concentration for intracellular LLPS. Full-length FLG (with 12 FLG repeats) readily undergoes LLPS at low intracellular levels (~2 μM). In contrast, common FLG truncation mutants (with $\leq$4 FLG repeats) essentially lose the ability to undergo intracellular LLPS, exhibiting exceedingly high critical concentrations for LLPS (~130 to >1,500 μM) (Quiroz et al., 2020). Before the onset of skin inflammation, *FLG* nonsense mutations do not severely alter *FLG* mRNA transcripts (Nirunsuksiri et al., 1995) or prevent their translation (Kawasaki et al., 2012; Manabe et al., 1991; Sandilands et al., 2007). Yet, KG assembly is consistently compromised, emphasizing the repeat-encoded LLPS of FLG. Losing their ability to undergo LLPS at low intracellular levels, FLG truncated mutants likely follow the fate of many soluble IDPs, becoming targets for degradation (van der Lee et al., 2014). Intriguingly, common nonsense *FLG* mutations that largely spare the repeat domain are also associated with AD (Figure 2b). Although FLG variants with >8 tandem FLG repeats drive KG assembly at low critical concentrations, removal of the tiny C-terminal tail domain (drawn to scale in Figure 2b)—a puzzling 26-residue sequence conserved across mammals (Presland et al., 1992; Sandilands et al., 2009)— decreases KG viscosity, switching KGs from nuclei deforming to nuclei wetting (Quiroz et al., 2020).

These LLPS-inspired observations suggest that the fine tuning of KG viscosity contributes to skin barrier formation. Notably, despite the lack of sequence conservation between mouse and human FLG, they share LLPS-specific compositional biases (Figure 2f) and assemble KGs of similar viscosity

(Quiroz et al., 2020). Contrary to expectation, de novo assembled KGs in cultured, poorly differentiated KCs are less viscous than native KGs in stratifying epidermis, suggesting that differentiation-associated proteins modulate in vivo KG-phase dynamics (Quiroz et al., 2020). Revisiting *FLG* nonsense mutations, mutants with increasingly larger truncations of the IDP domain, if permissive for KG assembly (e.g., downstream of mut-n4 in Figure 2b), assemble KG-like structures with progressive downward shifts in viscosity (Quiroz et al., 2020). A prediction follows that progressively N-terminal *FLG* mutations may lead to more severe skin barrier phenotypes. However, current genetic studies largely oversimplify FLG truncation as loss of function (Margolis et al., 2019).

This novel focus on KG-phase dynamics informs a new perspective to understand the role of FLG in skin barrier formation and its mutational landscape in skin barrier disorders. Arguably, the analysis of FLG truncations remains heavily influenced by the original focus on filaggrin. Mutations are interpreted and quantified as loss of processed FLG repeats in the corneum. A priori, capturing the disease severity of *FLG* genotypes requires the lens of epidermal LLPS dynamics. This view is relevant to interpreting skin phenotypes in humans with compound heterozygous *FLG* mutations, combining alleles with N-terminal and C-terminal FLG truncations (Sandilands et al., 2007). Similarly, although the protective effect of long FLG variants has been typically analyzed as a total sum of available FLG repeats across the two alleles, the lowest risk is already conferred by having one 12-repeat *FLG* allele (Margolis et al., 2020a). We propose that these complex genotype–phenotype relationships are rooted in the strong repeat-encoded LLPS behaviors of FLG proteins, which dictate KG-phase dynamics. As *FLG* genotyping continues to improve and expands beyond nonsense mutations (Margolis et al., 2020b, 2019; Zhu et al., 2021), we suggest refining the definition of *FLG* loss-of-function mutations to account for their impact on epidermal LLPS dynamics.

Outlook

The central role of KG-phase dynamics in skin barrier formation was presciently described by Dale et al. (1994) when they wrote that "packing and unpacking of keratohyalin granules, and the biochemical changes in the constituent proteins, will be revealed to be exquisitely adapted to this controlled cellular reorganization." Realizing this vision, through the lens of epidermal LLPS dynamics, KGs emerge as liquid-like membraneless organelles whose assembly and disassembly fuel skin barrier formation (Quiroz et al., 2020).

Building on this conceptual and experimental progress, our knowledge of KG-phase dynamics suggests new questions and approaches to crack the skin barrier at cellular and molecular levels. Traditionally studied as a cell death mechanism, the granular-to-corneum transition does not accomplish cell death per se, but the formation of the all-important functional skin barrier (Eckhart et al., 2013; Koenig et al., 2020). This mechanistic and functional distinction strongly motivates the adoption of corneoptosis (Matsui et al., 2021) as the preferred term to describe the early stages of corneocyte formation. Beyond a renewed focus on *FLG* mutations and profiling of KG clients through proximity-dependent proteomics, we propose four major directions to link LLPS dynamics with concurrent cellular processes at play in corneoptosis.

First, because environmental extremes uniquely act on the skin surface, we envision that future work will uncover the links between epidermal LLPS dynamics and the environmental resilience of the skin barrier. Because this resilience is lacking in humans with KG defects, these efforts may illuminate therapeutic avenues to address skin barrier disorders. As an example, cold temperatures and low humidity are linked to exacerbation of skin phenotypes in humans with AD (Engebretsen et al., 2016). Temperature fluctuations are relevant because the LLPS behavior of FLG-like IDPs is highly temperature sensitive (Quiroz and Chilkoti, 2015), and cells in the granular layer may experience skin temperature gradients. We suspect that temperature-dependent KG-phase dynamics contribute to the environmental responsiveness of the skin barrier.

Second, understanding the role of intracellular crowding will be critical to capturing the remarkable structural reorganizations associated with KG assembly, maturation, and disassembly. Macromolecular crowding of the intracellular space is emerging as a biophysical means of tuning cellular mechanisms (Delarue et al., 2018; Mourão et al., 2014). In a crowded cellular environment, the interaction between membraneless organelles and membrane-bound organelles merits attention. For example, in osteosarcoma cells in culture, ER exit sites closely interact with membraneless P-bodies to control their fusion and fission (Lee et al., 2020). In the skin, these potential organelle interactions may contribute to the overall cytoplasmic organization imposed by maturing KGs (Figure 3c) and its subsequent remodeling during KG dissolution. Abundant KGs may influence the morphology and function of the ER and other organelles as epidermal cells approach the granular-to-corneum transition. For example, potential KG–ER interactions could link the pH-triggered and KG-dependent dynamics of enucleation to the release of DNase1L2 from the ER. KG-induced crowding may serve as one of the missing stratification-specific regulators of the selective autophagic degradation and eventual loss of mitochondria (Simpson et al., 2021). Similarly, crowding with organized arrays of KGs may contribute to the scaffolding of the tubulo-reticular *trans*-Golgi network that mediates the barrier-defining secretion of membrane-bound lamellar bodies (Elias et al., 1998; Yamanishi et al., 2019). In addition to organelle interactions, KG crowding appears to influence the higher-order bundling of keratins (Figure 3c). Although the puzzling association between KGs and keratin fibers has long been documented through electron microscopy (Brody, 1959b), new experimental insights showed that IDP domains in KRT1 and KRT10 bind to FLG in KGs (Quiroz et al., 2020). Unable to enter FLG-rich KGs, K1/K10 fibers organize around KGs. We surmise that KG-interacting keratin fibers further pack and bundle as growing arrays of KGs exclude a larger volume of the cytoplasm. In line with this view, keratin network defects are already evident in the granular layer of *Flg*-null mice (Kawasaki et al., 2012; Usui et al., 2019). The collective evidence points to a role for growing KGs in orchestrating progressive keratin assembly

before FLG processing and corneoptosis. Future work should re-examine how KG disassembly, involving FLG processing and KG clients, impacts keratin bundling and reorganization of keratin fibers in the early corneocyte matrix (Iwai et al., 2012).

Third, uncovering the key molecular modulators of KG maturation and KG disassembly may offer new nodes to understand skin barrier formation and targets to address barrier disorders. The role of PTMs in governing KG disassembly is an obvious target for future research. The role of specific kinases in KG-phase dynamics deserves particular attention, but FLG proteolysis and arginine deimination through PADI3 are also relevant (Méchin et al., 2005; Nachat et al., 2005). The latter may also be at play in tuning the material properties of TGs (Ü Basmanav et al., 2016; Tarcsa et al., 1997). Regarding KG maturation, the potential role of FLG paralogs as drivers or modulators of epidermal LLPS behavior represents an exciting avenue for exploration, especially within the context of skin barrier disorders (Rahrig et al., 2019). Additional IDPs in the skin may also exhibit LLPS behavior. To offer a notable example, loricrin is a prototypical glycine-rich IDP (Candi et al., 2005) akin to LCST-exhibiting IDPs (Quiroz and Chilkoti, 2015). Loricrin changes substantially in length across species, concurrently shifting in subcellular localization. Mouse loricrin (486 residues) forms distinct membraneless granules in the granular layer but not in the human epidermis where loricrin (312 residues) resides in FLG-rich KGs (Yoneda et al., 1992). Given the prominent role of loricrin in epidermal differentiation (Candi et al., 2005), future work should examine how loricrin influences KG-phase dynamics and the reverse (how KGs impact loricrin function) in the human epidermis. Moreover, current efforts to explore FLG upregulation (Otsuka et al., 2014) and FLG fragments as therapeutic strategies (Cabanillas and Novak, 2016; Stout et al., 2014) may benefit from considering and targeting KG-phase dynamics.

Fourth, moving beyond KG-phase dynamics, epidermal biology may uniquely exploit intracellular LLPS dynamics at cell–cell junctions. We are intrigued by the recent discovery that tight junction proteins assemble through LLPS (Beutel et al., 2019). Although tight junction assembly plays a critical role in the skin barrier, the details of how epidermal cells restrict its assembly to the uppermost granular layer remain elusive. We also lack an understanding of how these junctions respond dynamically to environmental pressures on the skin barrier (Rübsam et al., 2017). Another example involves membraneless desmoplakin-containing particles in the assembly of epidermal desmosomes, which consist of dense protein clusters that anchor keratins to the plasma membranes at intercellular junctions (Godsel et al., 2005). The study of such biomolecular condensates at cell–cell junctions (Belardi et al., 2020) is an exciting direction for future research at the interface of LLPS and skin biology.

Finally, we foresee broad exploration of LLPS dynamics across epithelial terminal differentiation programs. Dissection of TG-phase dynamics represents an important direction for unraveling the remarkably complex process of terminal differentiation in hair formation. Given the prominent role of TGs in this process and the emergent genetic links between *TCHH* mutations and hair disorders (Ü Basmanav et al., 2016), this miniorgan offers an outstanding opportunity to probe physiologically relevant LLPS dynamics. Given the unique IDP-like architecture and composition of TCHH, TG-phase dynamics may differ substantially from KG-phase dynamics, offering an opportunity to uncover new features of in vivo LLPS dynamics. Overall, we hope that the updated view of KGs and TGs as epithelial membraneless organelles will inspire new efforts and approaches to dissect hitherto enigmatic cellular mechanisms in epithelial biology.

ORCIDs
Alexa Regina Chua Avecilla: http://orcid.org/0000-0001-6708-805X
Felipe Garcia Quiroz: http://orcid.org/0000-0001-6454-9615

AUTHOR CONTRIBUTIONS
Conceptualization: FGQ, ARCA; Data Curation: ARCA, FGQ; Funding Acquisition: FGQ; Visualization: ARCA, FGQ; Writing - Original Draft Preparation: ARCA, FGQ

ACKNOWLEDGMENTS
We thank Brian Long for assistance with our illustrations of epidermal liquid-liquid phase separation dynamics in Figure 3. We thank H. Amalia Pasolli at Rockefeller University (New York City, NY) for discussions on the ultrastructural features and localization of trichohyalin granules in mouse hair follicles. FGQ holds a Career Award at the Scientific Interface from Burroughs Wellcome Fund.

CONFLICT OF INTEREST
FGQ is an inventor on a United States patent application covering designs and uses of phase-separation sensors. The remaining author declares no conflict of interest.

REFERENCES
Albérola G, Schröder JM, Froment C, Simon M. The amino-terminal part of human FLG2 is a component of cornified envelopes. J Invest Dermatol 2019;139:1395–7.

Alberti S, Gladfelter A, Mittag T. Considerations and challenges in studying liquid-liquid phase separation and biomolecular condensates. Cell 2019;176:419–34.

Alef T, Torres S, Hausser I, Metze D, Türsen U, Lestringant GG, et al. Ichthyosis, follicular atrophoderma, and hypotrichosis caused by mutations in ST14 is associated with impaired profilaggrin processing. J Invest Dermatol 2009;129:862–9.

Alfares A, Al-Khenaizan S, Al Mutairi F. Peeling skin syndrome associated with novel variant in FLG2 gene. Am J Med Genet A 2017;173:3201–4.

Ambadipudi S, Biernat J, Riedel D, Mandelkow E, Zweckstetter M. Liquid–liquid phase separation of the microtubule-binding repeats of the Alzheimer-related protein Tau. Nat Commun 2017;8:275.

Banani SF, Lee HO, Hyman AA, Rosen MK. Biomolecular condensates: organizers of cellular biochemistry. Nat Rev Mol Cell Biol 2017;18:285–98.

Banani SF, Rice AM, Peeples WB, Lin Y, Jain S, Parker R, et al. Compositional control of phase-separated cellular bodies. Cell 2016;166:651–63.

Belardi B, Son S, Felce JH, Dustin ML, Fletcher DA. Cell–cell interfaces as specialized compartments directing cell function. Nat Rev Mol Cell Biol 2020;21:750–64.

Bergeron-Sandoval LP, Safaee N, Michnick SW. Mechanisms and consequences of macromolecular phase separation. Cell 2016;165:1067–79.

Beutel O, Maraspini R, Pombo-García K, Martin-Lemaitre C, Honigmann A. Phase separation of zonula occludens proteins drives formation of tight junctions. Cell 2019;179:923–36.e11.

Birbeck M, Mercer EH. The electron microscopy of the human hair follicle, III. The inner root sheath and trichohyaline. J Biophys Biochem Cytol 1957;3:223–30.

Bracha D, Walls MT, Brangwynne CP. Probing and engineering liquid-phase organelles. Nat Biotechnol 2019;37:1435–45.

Bracha D, Walls MT, Wei M-T, Zhu L, Kurian M, Avalos JL, et al. Mapping local and global liquid phase behavior in living cells using photo-oligomerizable seeds [published correction appears in Cell 2019;176:407]. Cell 2018;175:1467–80.e13.

Brangwynne CP, Tompa P, Pappu RV. Polymer physics of intracellular phase transitions. Nat Phys 2015;11:899–904.

Brangwynne CP, Eckmann CR, Courson DS, Rybarska A, Hoege C, Gharakhani J, et al. Germline P granules are liquid droplets that localize by controlled dissolution/condensation. Science 2009;324:1729–32.

Brangwynne CP, Mitchison TJ, Hyman AA. Active liquid-like behavior of nucleoli determines their size and shape in Xenopus laevis oocytes. Proc Natl Acad Sci USA 2011;108:4334–9.

Brody I. The keratinization of epidermal cells of normal guinea pig skin as revealed by electron microscopy. J Ultrastruct Res 1959a;2:482–511.

Brody I. An ultrastructural study on the role of the keratohyalin granules in the keratinization process. J Ultrastruct Res 1959b;3:84–104.

Brody I. Ultrastructure of the stratum corneum. Int J Dermatol 1977;16: 245–56.

Brown SJ, Kroboth K, Sandilands A, Campbell LE, Pohler E, Kezic S, et al. Intragenic copy number variation within filaggrin contributes to the risk of atopic dermatitis with a dose-dependent effect. J Invest Dermatol 2012;132:98–104.

Brown SJ, McLean WH. One remarkable molecule: filaggrin. J Invest Dermatol 2012;132:751–62.

Bunick CG, Presland RB, Lawrence OT, Pearton DJ, Milstone LM, Steitz TA. Crystal structure of human profilaggrin S100 domain and identification of target proteins annexin II, stratifin, and HSP27. J Invest Dermatol 2015;135: 1801–9.

Cabanillas B, Novak N. Atopic dermatitis and filaggrin. Curr Opin Immunol 2016;42:1–8.

Cajal SR. Un sencillo método de coloración selectiva del retículo protoplasmático y sus efectos en los diversos órganos nerviosos de vertebrados e invertebrados. Trab Lab Invest Biol Univ Madrid 1903;2:129–221.

Cajal SR. El núcleo de las células piramidales del cerebro humano y de algunos mamíferos. Trab Lab Invest Biol Univ Madrid 1910;8:27–62.

Candi E, Schmidt R, Melino G. The cornified envelope: a model of cell death in the skin. Nat Rev Mol Cell Biol 2005;6:328–40.

Cau L, Pendaries V, Lhuillier E, Thompson PR, Serre G, Takahara H, et al. Lowering relative humidity level increases epidermal protein deimination and drives human filaggrin breakdown. J Dermatol Sci 2017;86:106–13.

Chen H, Ho JC, Sandilands A, Chan YC, Giam YC, Evans AT, et al. Unique and recurrent mutations in the filaggrin gene in Singaporean Chinese patients with ichthyosis vulgaris [published correction appears in J Invest Dermatol 2008;128:2545]. J Invest Dermatol 2008;128:1669–75.

Dale BA. Purification and characterization of a basic protein from stratum corneum of mammalian epidermis. Biochim Biophys Acta 1977;491: 193–204.

Dale BA, Holbrook KA, Steinert PM. Assembly of stratum corneum basic protein and keratin filaments in macrofibrils. Nature 1978;276:729–31.

Dale BA, Presland RB, Lewis SP, Underwood RA, Fleckman P. Transient expression of epidermal filaggrin in cultured cells causes collapse of intermediate filament networks with alteration of cell shape and nuclear integrity. J Invest Dermatol 1997;108:179–87.

Dale BA, Resing KA, Presland RB. Keratohyalin granule proteins. In: Leigh I, Lane EB, Watt FM, editors. The keratinocyte handbook. New York, NY: Cambridge University Press; 1994. p. 323–50.

Das S, Lin YH, Vernon RM, Forman-Kay JD, Chan HS. Comparative roles of charge, π, and hydrophobic interactions in sequence-dependent phase separation of intrinsically disordered proteins. Proc Natl Acad Sci USA 2020;117:28795–805.

De Benedetto A, Qualia CM, Baroody FM, Beck LA. Filaggrin expression in oral, nasal, and esophageal mucosa. J Invest Dermatol 2008;128:1594–7.

de Guzman Strong C, Conlan S, Deming CB, Cheng J, Sears KE, Segre JA. A milieu of regulatory elements in the epidermal differentiation complex syntenic block: implications for atopic dermatitis and psoriasis. Hum Mol Genet 2010;19:1453–60.

Delarue M, Brittingham GP, Pfeffer S, Surovtsev IV, Pinglay S, Kennedy KJ, et al. mTORC1 controls phase separation and the biophysical properties of the cytoplasm by tuning crowding. Cell 2018;174:338–49.e20.

Denecker G, Hoste E, Gilbert B, Hochepied T, Ovaere P, Lippens S, et al. Caspase-14 protects against epidermal UVB photodamage and water loss. Nat Cell Biol 2007;9:666–74.

Dignon GL, Zheng W, Kim YC, Mittal J. Temperature-controlled liquid–liquid phase separation of disordered proteins. ACS Cent Sci 2019;5:821–30.

Dodson AE, Kennedy S. Phase separation in germ cells and development. Dev Cell 2020;55:4–17.

Dunker AK, Lawson JD, Brown CJ, Williams RM, Romero P, Oh JS, et al. Intrinsically disordered protein. J Mol Graph Model 2001;19:26–59.

Dzuricky M, Roberts S, Chilkoti A. Convergence of artificial protein polymers and intrinsically disordered proteins. Biochemistry 2018;57:2405–14.

Eckhart L, Lippens S, Tschachler E, Declercq W. Cell death by cornification. Biochim Biophys Acta 2013;1833:3471–80.

Elias PM, Cullander C, Mauro T, Rassner U, Kömüves L, Brown BE, et al. The secretory granular cell: the outermost granular cell as a specialized secretory cell. J Investig Dermatol Symp Proc 1998;3:87–100.

Engebretsen KA, Johansen JD, Kezic S, Linneberg A, Thyssen JP. The effect of environmental humidity and temperature on skin barrier function and dermatitis. J Eur Acad Dermatol Venereol 2016;30:223–49.

Fischer H, Buchberger M, Napirei M, Tschachler E, Eckhart L. Inactivation of DNase1L2 and DNase2 in keratinocytes suppresses DNA degradation during epidermal cornification and results in constitutive parakeratosis. Sci Rep 2017;7:6433.

Fischer H, Eckhart L, Mildner M, Jaeger K, Buchberger M, Ghannadan M, et al. DNase1L2 degrades nuclear DNA during corneocyte formation. J Invest Dermatol 2007;127:24–30.

Fischer H, Szabo S, Scherz J, Jaeger K, Rossiter H, Buchberger M, et al. Essential role of the keratinocyte-specific endonuclease DNase1L2 in the removal of nuclear DNA from hair and nails. J Invest Dermatol 2011;131: 1208–15.

Fuchs E. Scratching the surface of skin development. Nature 2007;445: 834–42.

Fukuyama K, Epstein WL. A comparative autoradiographic study of keratogyalin granules containing cystine and histidine. J Ultrastruct Res 1975;51: 314–25.

Fukuyama K, Nakamura T, Benstein IA. Differentially localized incorporation of amino acids in relation to epidermal keratinization in the newborn rat. Anat Rec 1965;152:525–35.

Gall JG. The centennial of the Cajal body. Nat Rev Mol Cell Biol 2003;4: 975–80.

Garcia-Jove Navarro M, Kashida S, Chouaib R, Souquere S, Pierron G, Weil D, et al. RNA is a critical element for the sizing and the composition of phase-separated RNA-protein condensates. Nat Commun 2019;10: 3230.

Godsel LM, Hsieh SN, Amargo EV, Bass AE, Pascoe-McGillicuddy LT, Huen AC, et al. Desmoplakin assembly dynamics in four dimensions: multiple phases differentially regulated by intermediate filaments and actin. J Cell Biol 2005;171:1045–59.

Hamilton EH, Payne RE Jr, O'keefe EJ. Trichohyalin: presence in the granular layer and stratum corneum of normal human epidermis. J Invest Dermatol 1991;96:666–72.

Hardenberg M, Horvath A, Ambrus V, Fuxreiter M, Vendruscolo M. Widespread occurrence of the droplet state of proteins in the human proteome. Proc Natl Acad Sci USA 2020;117:33254–62.

Harding CR, Scott IR. Histidine-rich proteins (filaggrins): structural and functional heterogeneity during epidermal differentiation. J Mol Biol 1983;170:651–73.

Hegner RW. Effects of removing the germ-cell determinants from the eggs of some chrysomelid beetles. Preliminary report. Biol Bull 1908;16:19–26.

Hegner RW. The germ cell determinants in the eggs of chrysomelid beetles. Science 1911;33:71–2.

Hinbest AJ, Kim SR, Eldirany SA, Lomakin IB, Watson J, Ho M, et al. Structural properties of target binding by profilaggrin A and B domains and other S100 fused-type calcium-binding proteins. J Dermatol Sci 2020;100: 39–49.

Holbrook KA. Biologic structure and function: perspectives on morphologic approaches to the study of the granular layer keratinocyte. J Invest Dermatol 1989;92(Suppl. 4):S84–104.

Hoste E, Kemperman P, Devos M, Denecker G, Kezic S, Yau N, et al. Caspase-14 is required for filaggrin degradation to natural moisturizing factors in the skin. J Invest Dermatol 2011;131:2233–41.

Hsu CY, Henry J, Raymond AA, Méchin MC, Pendaries V, Nassar D, et al. Deimination of human filaggrin-2 promotes its proteolysis by calpain 1. J Biol Chem 2011;286:23222–33.

Huber M, Siegenthaler G, Mirancea N, Marenholz I, Nizetic D, Breitkreutz D, et al. Isolation and characterization of human repetin, a member of the fused gene family of the epidermal differentiation complex. J Invest Dermatol 2005;124:998–1007.

Ipponjima S, Umino Y, Nagayama M, Denda M. Live imaging of alterations in cellular morphology and organelles during cornification using an epidermal equivalent model. Sci Rep 2020;10:5515.

Ishida-Yamamoto A, Eady RA, Underwood RA, Dale BA, Holbrook KA. Filaggrin expression in epidermolytic ichthyosis (epidermolytic hyperkeratosis). Br J Dermatol 1994;131:767–79.

Iwai I, Han H, den Hollander L, Svensson S, Ofverstedt LG, Anwar J, et al. The human skin barrier is organized as stacked bilayers of fully extended ceramides with cholesterol molecules associated with the ceramide sphingoid moiety. J Invest Dermatol 2012;132:2215–25.

Jain A, Vale RD. RNA phase transitions in repeat expansion disorders. Nature 2017;546:243–7.

Jawerth L, Fischer-Friedrich E, Saha S, Wang J, Franzmann T, Zhang X, et al. Protein condensates as aging Maxwell fluids. Science 2020;370:1317–23.

Jones DT, Cozzetto D. DISOPRED3: precise disordered region predictions with annotated protein-binding activity. Bioinformatics 2015;31:857–63.

Kamata Y, Taniguchi A, Yamamoto M, Nomura J, Ishihara K, Takahara H, et al. Neutral cysteine protease bleomycin hydrolase is essential for the breakdown of deiminated filaggrin into amino acids. J Biol Chem 2009;284:12829–36.

Kantor R, Silverberg JI. Environmental risk factors and their role in the management of atopic dermatitis. Expert Rev Clin Immunol 2017;13:15–26.

Karczewski KJ, Francioli LC, Tiao G, Cummings BB, Alföldi J, Wang Q, et al. The mutational constraint spectrum quantified from variation in 141,456 humans [published correction appears in Nature 2021;590:E53]. Nature 2020;581:434–43.

Kato M, Han TW, Xie S, Shi K, Du X, Wu LC, et al. Cell-free formation of RNA granules: low complexity sequence domains form dynamic fibers within hydrogels. Cell 2012;149:753–67.

Kaur T, Raju M, Alshareedah I, Davis RB, Potoyan DA, Banerjee PR. Sequence-encoded and composition-dependent protein-RNA interactions control multiphasic condensate morphologies. Nat Commun 2021;12:872.

Kawasaki H, Nagao K, Kubo A, Hata T, Shimizu A, Mizuno H, et al. Altered stratum corneum barrier and enhanced percutaneous immune responses in filaggrin-null mice. J Allergy Clin Immunol 2012;129:1538–46.e6.

Klosin A, Oltsch F, Harmon T, Honigmann A, Jülicher F, Hyman AA, et al. Phase separation provides a mechanism to reduce noise in cells. Science 2020;367:464–8.

Koenig U, Robenek H, Barresi C, Brandstetter M, Resch GP, Gröger M, et al. Cell death induced autophagy contributes to terminal differentiation of skin and skin appendages. Autophagy 2020;16:932–45.

Krieg P, Schuppler M, Koesters R, Mincheva A, Lichter P, Marks F. Repetin (Rptn), a new member of the "fused gene" subgroup within the S100 gene family encoding a murine epidermal differentiation protein. Genomics 1997;43:339–48.

Kubo A, Nagao K, Amagai M. Epidermal barrier dysfunction and cutaneous sensitization in atopic diseases. J Clin Invest 2012;122:440–7.

Kumar V, Bouameur JE, Bär J, Rice RH, Hornig-Do HT, Roop DR, et al. A keratin scaffold regulates epidermal barrier formation, mitochondrial lipid composition, and activity [published correction appears in J Cell Biol 2016;212:877]. J Cell Biol 2015;211:1057–75.

Lamond AI, Spector DL. Nuclear speckles: a model for nuclear organelles. Nat Rev Mol Cell Biol 2003;4:605–12.

Langdon EM, Qiu Y, Ghanbari Niaki AG, McLaughlin GA, Weidmann CA, Gerbich TM, et al. mRNA structure determines specificity of a polyQ-driven phase separation. Science 2018;360:922–7.

Lavker RM, Matoltsy AG. Substructure of keratohyalin granules of the epidermis as revealed by high resolution electron microscopy. J Ultrastruct Res 1971;35:575–81.

Leblond CP. The life history of cells in renewing systems. Am J Anat 1981;160:114–58.

Lee JE, Cathey PI, Wu H, Parker R, Voeltz GK. Endoplasmic reticulum contact sites regulate the dynamics of membraneless organelles. Science 2020;367:eaay7108.

Lee SC, Kim IG, Marekov LN, O'keefe EJ, Parry DA, Steinert PM. The structure of human trichohyalin. Potential multiple roles as a functional EF-hand-like calcium-binding protein, a cornified cell envelope precursor, and an intermediate filament-associated (cross-linking) protein. J Biol Chem 1993;268:12164–76.

Leyvraz CL, Charles RP, Rubera I, Guitard M, Rotman S, Breiden B, et al. The epidermal barrier function is dependent on the serine protease CAP1/Prss8. J Cell Biol 2005;170:487–96.

Li P, Banjade S, Cheng HC, Kim S, Chen B, Guo L, et al. Phase transitions in the assembly of multivalent signalling proteins. Nature 2012;483:336–40.

List K, Szabo R, Wertz PW, Segre J, Haudenschild CC, Kim SY, et al. Loss of proteolytically processed filaggrin caused by epidermal deletion of matriptase/MT-SP1. J Cell Biol 2003;163:901–10.

Lonsdale-Eccles JD, Haugen JA, Dale BA. A phosphorylated keratohyalin-derived precursor of epidermal stratum corneum basic protein. J Biol Chem 1980;255:2235–8.

Lonsdale-Eccles JD, Teller DC, Dale BA. Characterization of a phosphorylated form of the intermediate filament-aggregating protein filaggrin. Biochemistry 1982;21:5940–8.

Madison KC. Barrier function of the skin: "la raison d'etre" of the epidermis. J Invest Dermatol 2003;121:231–41.

Mahowald AP. Fine structure of pole cells and polar granules in Drosophila melanogaster. J Exp Zool 1962;151:201–15.

Makino T, Takaishi M, Morohashi M, Huh NH. Hornerin, a novel profilaggrin-like protein and differentiation-specific marker isolated from mouse skin. J Biol Chem 2001;276:47445–52.

Manabe M, O'Guin WM. Existence of trichohyalin-keratohyalin hybrid granules: co-localization of two major intermediate filament-associated proteins in non-follicular epithelia. Differentiation 1994;58:65–75.

Manabe M, Sanchez M, Sun TT, Dale BA. Interaction of filaggrin with keratin filaments during advanced stages of normal human epidermal differentiation and in ichthyosis vulgaris. Differentiation 1991;48:43–50.

Margolis DJ, Gupta J, Apter AJ, Ganguly T, Hoffstad O, Papadopoulos M, et al. Filaggrin-2 variation is associated with more persistent atopic dermatitis in African American subjects. J Allergy Clin Immunol 2014;133:784–9.

Margolis DJ, Mitra N, Berna R, Hoffstad O, Kim BS, Yan A, et al. Associating filaggrin copy number variation and atopic dermatitis in African-Americans: challenges and opportunities. J Dermatol Sci 2020a;98:58–60.

Margolis DJ, Mitra N, Wubbenhorst B, D'Andrea K, Kraya AA, Hoffstad O, et al. Association of filaggrin loss-of-function variants with race in children with atopic dermatitis. JAMA Dermatol 2019;155:1269–76.

Margolis DJ, Mitra N, Wubbenhorst B, Nathanson KL. Filaggrin sequencing and bioinformatics tools. Arch Dermatol Res 2020b;312:155–8.

Markmiller S, Soltanieh S, Server KL, Mak R, Jin W, Fang MY, et al. Context-dependent and disease-specific diversity in protein interactions within stress granules. Cell 2018;172:590–604.e13.

Martins AF, Bennett NC, Clavel S, Groenewald H, Hensman S, Hoby S, et al. Locally-curved geometry generates bending cracks in the African elephant skin. Nat Commun 2018;9:3865.

Matoltsy AG, Matoltsy MN. The chemical nature of keratohyalin granules of the epidermis. J Cell Biol 1970;47:593–603.

Matsui T, Kadono-Maekubo N, Suzuki Y, Furuichi Y, Shiraga K, Sasaki H, et al. A unique mode of keratinocyte death requires intracellular acidification. Proc Natl Acad Sci USA 2021;118:e2020722118.

Matsui T, Kinoshita-Ida Y, Hayashi-Kisumi F, Hata M, Matsubara K, Chiba M, et al. Mouse homologue of skin-specific retroviral-like aspartic protease involved in wrinkle formation. J Biol Chem 2006;281:27512–25.

Matsui T, Miyamoto K, Kubo A, Kawasaki H, Ebihara T, Hata K, et al. SASPase regulates stratum corneum hydration through profilaggrin-to-filaggrin processing. EMBO Mol Med 2011;3:320–33.

Méchin MC, Enji M, Nachat R, Chavanas S, Charveron M, Ishida-Yamamoto A, et al. The peptidylarginine deiminases expressed in human epidermis differ in their substrate specificities and subcellular locations. Cell Mol Life Sci 2005;62:1984–95.

Mischke D, Korge BP, Marenholz I, Volz A, Ziegler A. Genes encoding structural proteins of epidermal cornification and S100 calcium-binding proteins form a gene complex ("epidermal differentiation complex") on human chromosome 1q21. J Invest Dermatol 1996;106:989–92.

Mlitz V, Latreille J, Gardinier S, Jdid R, Drouault Y, Hufnagl P, et al. Impact of filaggrin mutations on Raman spectra and biophysical properties of the stratum corneum in mild to moderate atopic dermatitis. J Eur Acad Dermatol Venereol 2012;26:983–90.

Mohamad J, Sarig O, Godsel LM, Peled A, Malchin N, Bochner R, et al. Filaggrin 2 deficiency results in abnormal cell-cell adhesion in the cornified cell layers and causes peeling skin syndrome type A. J Invest Dermatol 2018;138:1736–43.

Moreci RS, Lechler T. Epidermal structure and differentiation. Curr Biol 2020;30:R144–9.

Mourão MA, Hakim JB, Schnell S. Connecting the dots: the effects of macromolecular crowding on cell physiology. Biophys J 2014;107:2761–6.

Nachat R, Méchin MC, Takahara H, Chavanas S, Charveron M, Serre G, et al. Peptidylarginine deiminase isoforms 1–3 are expressed in the epidermis and involved in the deimination of K1 and filaggrin. J Invest Dermatol 2005;124:384–93.

Narangifard A, Wennberg CL, den Hollander L, Iwai I, Han H, Lundborg M, et al. Molecular reorganization during formation of the human skin barrier studied in situ. J Invest Dermatol 2021;141:1243–53.e6.

Netzel-Arnett S, Currie BM, Szabo R, Lin CY, Chen LM, Chai KX, et al. Evidence for a matriptase-prostasin proteolytic cascade regulating terminal epidermal differentiation. J Biol Chem 2006;281:32941–5.

Nirunsuksiri W, Presland RB, Brumbaugh SG, Dale BA, Fleckman P. Decreased profilaggrin expression in ichthyosis vulgaris is a result of selectively impaired posttranscriptional control. J Biol Chem 1995;270:871–6.

Nomura T, Sandilands A, Akiyama M, Liao H, Evans AT, Sakai K, et al. Unique mutations in the filaggrin gene in Japanese patients with ichthyosis vulgaris and atopic dermatitis. J Allergy Clin Immunol 2007;119:434–40.

Nott TJ, Petsalaki E, Farber P, Jervis D, Fussner E, Plochowietz A, et al. Phase transition of a disordered nuage protein generates environmentally responsive membraneless organelles. Mol Cell 2015;57:936–47.

O'Guin WM, Sun TT, Manabe M. Interaction of trichohyalin with intermediate filaments: three immunologically defined stages of trichohyalin maturation. J Invest Dermatol 1992;98:24–32.

O'Keefe EJ, Hamilton EH, Lee SC, Steinert P. Trichohyalin: a structural protein of hair, tongue, nail, and epidermis. J Invest Dermatol 1993;101(Suppl. 1):S65–71.

Otsuka A, Doi H, Egawa G, Maekawa A, Fujita T, Nakamizo S, et al. Possible new therapeutic strategy to regulate atopic dermatitis through upregulating filaggrin expression. J Allergy Clin Immunol 2014;133:139–46.e1–10.

Owen I, Shewmaker F. The role of post-translational modifications in the phase transitions of intrinsically disordered proteins. Int J Mol Sci 2019;20:5501.

Palmer CN, Irvine AD, Terron-Kwiatkowski A, Zhao Y, Liao H, Lee SP, et al. Common loss-of-function variants of the epidermal barrier protein filaggrin are a major predisposing factor for atopic dermatitis. Nat Genet 2006;38:441–6.

Pasparakis M, Haase I, Nestle FO. Mechanisms regulating skin immunity and inflammation. Nat Rev Immunol 2014;14:289–301.

Pattanaik A, Gowda DC, Urry DW. Phosphorylation and dephosphorylation modulation of an inverse temperature transition. Biochem Biophys Res Commun 1991;178:539–45.

Pendaries V, Le Lamer M, Cau L, Hansmann B, Malaisse J, Kezic S, et al. In a three-dimensional reconstructed human epidermis filaggrin-2 is essential for proper cornification. Cell Death Dis 2015;6:e1656.

Presland RB, Haydock PV, Fleckman P, Nirunsuksiri W, Dale BA. Characterization of the human epidermal profilaggrin gene. Genomic organization and identification of an S-100-like calcium binding domain at the amino terminus. J Biol Chem 1992;267:23772–81.

Presland RB, Kimball JR, Kautsky MB, Lewis SP, Lo CY, Dale BA. Evidence for specific proteolytic cleavage of the N-terminal domain of human profilaggrin during epidermal differentiation. J Invest Dermatol 1997;108:170–8.

Quiroz FG, Chilkoti A. The language of protein polymers. In: Lutz JF, Meyer TY, Ouchi M, Sawamoto M, editors. Sequence-controlled polymers: synthesis, self-assembly, and properties, vol. 1170. Washington, DC: ACS Publications; 2014. p. 15–33.

Quiroz FG, Chilkoti A. Sequence heuristics to encode phase behaviour in intrinsically disordered protein polymers. Nat Mater 2015;14:1164–71.

Quiroz FG, Fiore VF, Levorse JM, Polak L, Wong E, Pasolli HA, et al. Liquid-liquid phase separation drives skin barrier formation. Science 2020;367:eaax9554.

Quiroz FG, Li NK, Roberts S, Weber P, Dzuricky M, Weitzhandler I, et al. Intrinsically disordered proteins access a range of hysteretic phase separation behaviors. Sci Adv 2019;5:eaax5177.

Rahrig S, Dettmann JM, Brauns B, Lorenz VN, Buhl T, Kezic S, et al. Transient epidermal barrier deficiency and lowered allergic threshold in filaggrin-hornerin (FlgHrnr$^{-/-}$) double-deficient mice. Allergy 2019;74:1327–39.

Resing KA, Johnson RS, Walsh KA. Characterization of protease processing sites during conversion of rat profilaggrin to filaggrin. Biochemistry 1993;32:10036–45.

Resing KA, Walsh KA, Dale BA. Identification of two intermediates during processing of profilaggrin to filaggrin in neonatal mouse epidermis. J Cell Biol 1984;99:1372–8.

Riback JA, Katanski CD, Kear-Scott JL, Pilipenko EV, Rojek AE, Sosnick TR, et al. Stress-triggered phase separation is an adaptive, evolutionarily tuned response. Cell 2017;168:1028–40.e19.

Riback JA, Zhu L, Ferrolino MC, Tolbert M, Mitrea DM, Sanders DW, et al. Composition-dependent thermodynamics of intracellular phase separation. Nature 2020;581:209–14.

Rogers GE. Isolation and properties of inner sheath cells of hair follicles. Exp Cell Res 1964;33:264–76.

Rompolas P, Mesa KR, Kawaguchi K, Park S, Gonzalez D, Brown S, et al. Spatiotemporal coordination of stem cell commitment during epidermal homeostasis. Science 2016;352:1471–4.

Rothnagel JA, Rogers GE. Trichohyalin, an intermediate filament-associated protein of the hair follicle. J Cell Biol 1986;102:1419–29.

Rübsam M, Mertz AF, Kubo A, Marg S, Jüngst C, Goranci-Buzhala G, et al. E-cadherin integrates mechanotransduction and EGFR signaling to control junctional tissue polarization and tight junction positioning. Nat Commun 2017;8:1250.

Sanders DW, Kedersha N, Lee DSW, Strom AR, Drake V, Riback JA, et al. Competing protein-RNA interaction networks control multiphase intracellular organization. Cell 2020;181:306–24.e28.

Sandilands A, Sutherland C, Irvine AD, McLean WH. Filaggrin in the frontline: role in skin barrier function and disease. J Cell Sci 2009;122:1285–94.

Sandilands A, Terron-Kwiatkowski A, Hull PR, O'Regan GM, Clayton TH, Watson RM, et al. Comprehensive analysis of the gene encoding filaggrin uncovers prevalent and rare mutations in ichthyosis vulgaris and atopic eczema. Nat Genet 2007;39:650–4.

Sawyer IA, Sturgill DM, Dundr M. Membraneless nuclear organelles and the search for phases within phases. Wiley Interdiscip Rev RNA 2019;10:e1514.

Scott IR, Harding CR. Filaggrin breakdown to water binding compounds during development of the rat stratum corneum is controlled by the water activity of the environment. Dev Biol 1986;115:84–92.

Scott IR, Harding CR, Barrett JG. Histidine-rich protein of the keratohyalin granules. Source of the free amino acids, urocanic acid and pyrrolidone carboxylic acid in the stratum corneum. Biochim Biophys Acta 1982;719:110–7.

Sender R, Milo R. The distribution of cellular turnover in the human body. Nat Med 2021;27:45–8.

Shin Y, Brangwynne CP. Liquid phase condensation in cell physiology and disease. Science 2017;357:eaaf4382.

Shiokawa D, Tanuma S. Characterization of human DNase I family endonucleases and activation of DNase gamma during apoptosis. Biochemistry 2001;40:143–52.

Simon M, Haftek M, Sebbag M, Montézin M, Girbal-Neuhauser E, Schmitt D, et al. Evidence that filaggrin is a component of cornified cell envelopes in human plantar epidermis. Biochem J 1996;317:173–7.

Simpson CL, Tokito MK, Uppala R, Sarkar MK, Gudjonsson JE, Holzbaur ELF. NIX initiates mitochondrial fragmentation via DRP1 to drive epidermal differentiation. Cell Rep 2021;34:108689.

Smith FJ, Irvine AD, Terron-Kwiatkowski A, Sandilands A, Campbell LE, Zhao Y, et al. Loss-of-function mutations in the gene encoding filaggrin cause ichthyosis vulgaris. Nat Genet 2006;38:337–42.

Smith SA, Dale BA. Immunologic localization of filaggrin in human oral epithelia and correlation with keratinization. J Invest Dermatol 1986;86: 168–72.

Steinert PM, Cantieri JS, Teller DC, Lonsdale-Eccles JD, Dale BA. Characterization of a class of cationic proteins that specifically interact with intermediate filaments. Proc Natl Acad Sci USA 1981;78:4097–101.

Steinert PM, Parry DA, Marekov LN. Trichohyalin mechanically strengthens the hair follicle: multiple cross-bridging roles in the inner root sheath. J Biol Chem 2003;278:41409–19.

Stout TE, McFarland T, Mitchell JC, Appukuttan B, Timothy Stout J. Recombinant filaggrin is internalized and processed to correct filaggrin deficiency. J Invest Dermatol 2014;134:423–9.

Strome S, Wood WB. Immunofluorescence visualization of germ-line-specific cytoplasmic granules in embryos, larvae, and adults of Caenorhabditis elegans. Proc Natl Acad Sci USA 1982;79:1558–62.

Su X, Ditlev JA, Hui E, Xing W, Banjade S, Okrut J, et al. Phase separation of signaling molecules promotes T cell receptor signal transduction. Science 2016;352:595–9.

Sybert VP, Dale BA, Holbrook KA. Ichthyosis vulgaris: identification of a defect in synthesis of filaggrin correlated with an absence of keratohyaline granules. J Invest Dermatol 1985;84:191–4.

Tarcsa E, Marekov LN, Andreoli J, Idler WW, Candi E, Chung SI, et al. The fate of trichohyalin. Sequential post-translational modifications by peptidylarginine deiminase and transglutaminases. J Biol Chem 1997;272: 27893–901.

Thyssen JP, Jakasa I, Riethmüller C, Schön MP, Braun A, Haftek M, et al. Filaggrin expression and processing deficiencies impair corneocyte surface texture and stiffness in mice. J Invest Dermatol 2020;140:615–23.e5.

Trinkle-Mulcahy L. Nucleolus: the consummate nuclear body. In: Lavelle C, Victor JM, editors. Nuclear architecture and dynamics. Translational epigenetics, vol. 2. The Netherlands: Elsevier; 2018. p. 257–82.

Ü Basmanav FB, Cau L, Tafazzoli A, Méchin MC, Wolf S, Romano MT, et al. Mutations in three genes encoding proteins involved in hair shaft formation cause uncombable hair syndrome. Am J Hum Genet 2016;99:1292–304.

Urry DW, Long MM, Cox BA, Ohnishi T, Mitchell LW, Jacobs M. The synthetic polypentapeptide of elastin coacervates and forms filamentous aggregates. Biochim Biophys Acta 1974;371:597–602.

Urry DW, Starcher B, Partridge SM. Coacervation of Solubilized elastin effects a notable conformational change. Nature 1969;222:795–6.

Usui K, Kadono N, Furuichi Y, Shiraga K, Saitou T, Kawasaki H, et al. 3D in vivo imaging of the keratin filament network in the mouse stratum granulosum reveals profilaggrin-dependent regulation of keratin bundling. J Dermatol Sci 2019;94:346–9.

van der Lee R, Buljan M, Lang B, Weatheritt RJ, Daughdrill GW, Dunker AK, et al. Classification of intrinsically disordered regions and proteins. Chem Rev 2014;114:6589–631.

Wang J, Choi JM, Holehouse AS, Lee HO, Zhang X, Jahnel M, et al. A molecular grammar governing the driving forces for phase separation of prion-like RNA binding proteins. Cell 2018;174:688–99.e16.

Wang JT, Smith J, Chen BC, Schmidt H, Rasoloson D, Paix A, et al. Regulation of RNA granule dynamics by phosphorylation of serine-rich, intrinsically disordered proteins in C. elegans. Elife 2014;3:e04591.

Wei MT, Elbaum-Garfinkle S, Holehouse AS, Chen CC, Feric M, Arnold CB, et al. Phase behaviour of disordered proteins underlying low density and high permeability of liquid organelles. Nat Chem 2017;9: 1118–25.

Wilson EB. The structure of protoplasm. Science 1899;10:33–45.

Winsor T, Burch GE. Differential roles of layers of human epigastric skin on diffusion rate of water. Arch Intern Med 1944;74:428–36.

Wong XFCC, Denil SLIJ, Foo JN, Chen H, Tay ASL, Haines RL, et al. Array-based sequencing of filaggrin gene for comprehensive detection of disease-associated variants. J Allergy Clin Immunol 2018;141:814–6.

Wright PE, Dyson HJ. Intrinsically disordered proteins in cellular signalling and regulation. Nat Rev Mol Cell Biol 2015;16:18–29.

Wu Z, Hansmann B, Meyer-Hoffert U, Gläser R, Schröder JM. Molecular identification and expression analysis of filaggrin-2, a member of the S100 fused-type protein family. PLoS One 2009a;4:e5227.

Wu Z, Meyer-Hoffert U, Reithmayer K, Paus R, Hansmann B, He Y, et al. Highly complex peptide aggregates of the S100 fused-type protein hornerin are present in human skin. J Invest Dermatol 2009b;129: 1446–58.

Yamanishi H, Soma T, Kishimoto J, Hibino T, Ishida-Yamamoto A. Marked changes in lamellar granule and trans-Golgi network structure occur during epidermal keratinocyte differentiation. J Invest Dermatol 2019;139: 352–9.

Yang F, Waters KM, Webb-Robertson BJ, Sowa MB, von Neubeck C, Aldrich JT, et al. Quantitative phosphoproteomics identifies filaggrin and other targets of ionizing radiation in a human skin model. Exp Dermatol 2012;21:352–7.

Yang H, Adam RC, Ge Y, Hua ZL, Fuchs E. Epithelial-mesenchymal micro-niches govern stem cell lineage choices. Cell 2017;169:483–96.e13.

Yang P, Mathieu C, Kolaitis RM, Zhang P, Messing J, Yurtsever U, et al. G3BP1 is a tunable switch that triggers phase separation to assemble stress granules. Cell 2020;181:325–45.e28.

Yokouchi M, Atsugi T, Logtestijn MV, Tanaka RJ, Kajimura M, Suematsu M, et al. Epidermal cell turnover across tight junctions based on Kelvin's tetrakaidecahedron cell shape. Elife 2016;5:e19593.

Yoneda K, Hohl D, McBride OW, Wang M, Cehrs KU, Idler WW, et al. The human loricrin gene. J Biol Chem 1992;267:18060–6.

Zhu Y, Mitra N, Feng Y, Tishkoff S, Hoffstad O, Margolis D. FLG variation differs between European Americans and African Americans. J Invest Dermatol 2021;141:1855–7.